钟福平, 钟建华, 艾合买提江·阿不都热合曼, 等. 华北克拉通破坏时间与破坏范围分布特征——来自银根—额济纳旗盆地苏红图坳陷早白垩世火山岩的启示[J]. 中国地质, 2015, 42(2): 435−456.
Zhong Fuping, Zhong Jianhua, Ahmatjan Abdurahman, et al. Timing and scale of the destruction of the North China craton: Revelation from the Early Cretaceous volcanic rocks in Suhongtu Depression of Inggen−Ejin Banner Basin[J]. Geology in China, 2015, 42(2): 435−456(in Chinese with English abstract).

华北克拉通破坏时间与破坏范围分布特征——来自银根—额济纳旗盆地苏红图坳陷早白垩世火山岩的启示

钟福平[1,2,3] 钟建华[4,5] 艾合买提江·阿不都热合曼[6] 王 毅[6] 由伟丰[6] 杨伟利[6]

（1.河南理工大学安全科学与工程学院瓦斯地质研究所，河南 焦作 454003；2.中原经济区煤层（页岩）气河南省协同创新中心，河南焦作 454000；3.河南省瓦斯地质与瓦斯治理重点实验室—省部共建国家重点实验室培育基地，河南 焦作 454003；4.中国石油大学（华东）地球资源与信息学院，山东 东营 257061；5.中国科学院广州地球化学研究所，广东 广州 510640；6.中国石油化工有限公司石油勘探开发研究院，北京 100083）

提要：克拉通破坏的时间和范围是华北克拉通破坏研究的重要基础问题，但是在华北克拉通破坏时间与破坏范围的问题上存在着不同观点。本文通过对位于华北克拉通西北部银根—额济纳旗盆地苏红图坳陷内采集的火山岩进行年代学及地球化学研究，认为苏红图火山岩年龄为105~113 Ma，为一套钾质碱性系列玄武岩，其形成机制是由于岩石圈发生减薄，软流圈地幔岩浆上涌，经分离结晶而形成的，而动力学机制主要是由于西伯利亚板块、内蒙古褶皱带和华北板块在晚侏罗世发生的碰撞拼合。此外，本文还在前人对华北克拉通破坏研究基础上，依据作者对苏红图坳陷火山岩做的一些工作，粗浅地探讨了华北克拉通破坏的时间与范围的问题，认为华北克拉通周缘均为构造薄弱带，北缘为兴—蒙造山带，南侧为大别—秦岭造山带，东侧为苏鲁带和太平洋俯冲带，河套裂陷、汾渭裂陷分别与古元古代高温变质孔兹岩带及约18.5亿年前华北克拉通东、西部块体拼合时形成的中部造山带内位置大致重合，而苏红图坳陷位于中亚造山带南缘，同时也处于两板块拼合交汇处。这些构造薄弱带处在不同时期发生的俯冲与碰撞的结合部位，它们可能是岩石圈减薄的起始位置，并且它们的俯冲与碰撞时间是华北克拉通破坏的起始时间。克拉通破坏范围主要发生在太行山以东地区，太行山以西的河套裂陷、汾渭裂陷发生了减薄，而苏红图坳陷在早白垩世也发生减薄，所以，破坏范围分布在地理上呈不连续分布特征，造成这种分布特征的主要原因是由于不同区域的破坏时间与破坏的动力学机制不同。

关 键 词：华北克拉通；银根—额济纳旗盆地苏红图坳陷；破坏范围；动力学机制

中图分类号：P583；P552；P56 **文献标志码**：A **文章编号**：1000−3657(2015)02−0435−22

Timing and scale of the destruction of the North China craton: Revelation from the Early Cretaceous volcanic rocks in Suhongtu Depression of Inggen−Ejin Banner Basin

收稿日期：2014−04−11；**改回日期**：2014−08−16

基金项目：国家科技重大专项“大型油气田及煤层气开发”（2011ZX05040）、“中国西北地区构造-岩相古地理研究与编图”（YPH08107）、长江学者和创新团队发展计划资助（IRT1235）及河南理工大学博士基金（B2012−109）联合资助。

作者简介：钟福平，男，1978年生，博士后，讲师，从事构造地质学科研与教学工作；E−mail：zhongfp@hpu.edu.cn。

ZHONG Fu-ping[1,2,3], ZHONG Jian-hua[4,5], Ahmatjan Abdurahman[6], WANG Yi[6], YOU Wei-feng[6], YANG Wei-li[6]

(1. *School of Safety Science and Engineering, Henan Polytechnic University, Jiaozuo* 454003*, Henan, China; 2. Collaborative Innovation Center of Coalbed Methane and Shale Gas for Central Plains Economic Region*，*Jiaozuo* 454003*, Henan, China;* 3. *State Key Laboratory Cultivation Base for Gas Geology and Gas Control, Henan Polytechnic University, Jiaozuo* 454003*, Henan, China;* 4. *Institute of Earth Resources and Information, University of Petroleum (East China), Dongying* 257061*, Shandong, China;* 5. *Guangzhou Institute of Geochemistry, Chinese Academy of Sciences, Guangzhou* 510640*, Guangdong, China;* 6. *Research Institute of Exploration and Development, China Petroleum and Chemical Corporation, Beijing* 100083*, China*)

Abstract: Suhongtu Depression in Inggen-Ejin Banner basin is located on the northwestern margin of the North China Craton. The periphery of the North China Craton is a weak tectonic belt, with Hing - Mongolian orogenic zone on the northern margin, Dabie - Qinling orogenic belt on the southern margin, Tan-Lu fracture zone and Pacific subduction zone on the eastern margin. Hetao rift and Fenwei rift are roughly coincident with positions of Paleoproterozoic high-temperature metamorphic rocks and the central orogenic belts, which were formed during the breakup period of the North China Craton and western blocks approximately 1.85 billion years ago. However, Suhongtu Depression is located on the southern edge of the Central Asia Orogenic Belt, and also lies at the junction of two plates. These structural weakness belts experienced subduction in different periods, and might have served as the starting locations of lithospheric thinning, and the time of their subduction and collision was the beginning of the destruction of the North China Craton. Craton destruction regions occurred mainly to the east of the Taihang Mountains, whereas thinning happened in Fenwei rift, Hetao rift and Suhongtu Depression west of the Taihang Mountains. Therefore, damages to the Suhongtu Depression lithosphere occurred on the northwest margin of the North China Craton in the late Early Cretaceous (~ 110Ma), and hence the damaged regions in the Craton were distributed discontinuously in geography, which resulted from different destruction periods and dynamic mechanisms of the lithosphere in different regions.

Key words: Suhongtu depression of Inggen-Ejin Banner Basin; North China Craton; destruction time; destruction range; dynamic mechanism

About the first author：ZHONG Fu-ping, male, post-doctoral, lecturer, born in 1978, majors in teaching and research work of structural geology; E-mail: zhongfp@hpu.edu.cn.

银根—额济纳旗盆地（以下简称银—额盆地）苏红图坳陷位于华北板块西北部，同时又处于中亚造山带南缘，塔里木地块与华北板块的交汇处（图1），构造背景复杂。盆地内火山岩发育3期，其中早白垩世晚期火山岩活动最为强烈，波及面较广，由中基性火山熔岩组成，产于下白垩统苏红图组中。银—额盆地是中国具有一定勘探潜力的含油气盆地[1]，而火山岩对油气的生成、运移和储存具有重要影响[2-3]。已有学者对该区早白垩世火山岩做过研究，并进行过一些有益的探索[4-7]。

华北克拉通以发育古老岩石和中生代岩石圈巨量减薄闻名于世，是世界上少有的遭受破坏及岩石圈巨量减薄的克拉通。20世纪初翁文灏先生[8]提出了燕山运动概念，随后陈国达先生[9]提出“地台活化”观点，在此基础上，20世纪90年代中外科学家提出的“岩石圈减薄”[10-11]或“去根”[12]的概念。随着研究的不断深入，人们逐步意识到克拉通东部不仅发生了巨厚岩石圈地幔的丢失，而且岩石圈地幔物质成分、热状态和流变学性质等方面发生了根本性的改变[13]。破坏和减薄伴随着一系列强烈的构造作用、岩浆作用、成矿大爆发及大型含油气盆地的形成，在全球极为少见，因此，华北克拉通成了近年来国内外研究的最热门课题之一。

克拉通破坏的时间和范围是华北克拉通破坏研究的重要基础问题，它的确定是探索克拉通破坏机制及其动力学控制因素的关键[14]。目前，在华北克拉通破坏发生的时间上存在着在石炭纪[15,16]、三叠纪[17,18]、侏罗纪[19-21]、白垩纪[22]和新生代[23]等不同的认识，而其破坏范围主要发生在华北克拉通东部，即太行山断裂带以东地区，但在太行山以西的汾渭

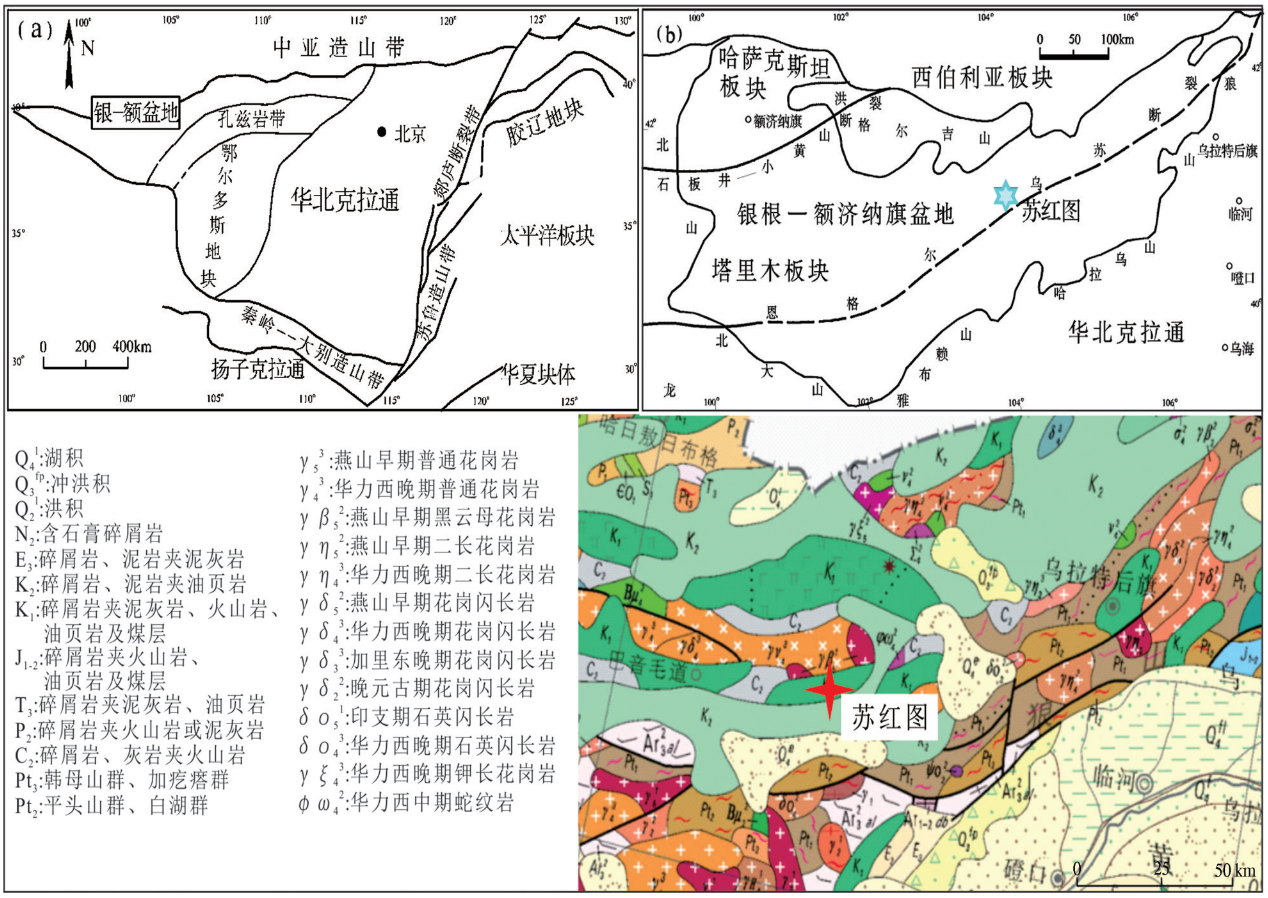

图1 样品采样位置图

Fig.1 Geographic map showing sampling sites

地堑、河套地堑下伏岩石圈也发生了减薄[24]。

通过对华北地区岩浆岩的研究，可以探讨华北克拉通破坏时间和范围。本文通过对银—额盆地苏红图坳陷早白垩世火山岩研究，探讨火山岩的地球化学特征及喷发动力学机制，依据苏红图坳陷大地构造位置特殊性，通过对华北克拉通发生破坏的时间和范围的探讨，结合对研究区火山岩年代学及动力学研究，探讨华北克拉通破坏范围分布特征，对于华北克拉通破坏研究具有重要意义。

1　苏红图火山岩年代学及地球化学特征

1.1 火山岩年代学

笔者在银—额盆地苏红图坳陷进行野外踏勘(图1~3)时采集大量火山岩样品，选送其中的6件样品（编号分别为Sht08、Sht11、Sht16、Sht18、Sht23、Sht28）进行 $^{40}Ar/^{39}Ar$ 定年，得到年龄值为105~113 Ma(表1，图4)。

$^{40}Ar/^{39}Ar$ 同位素定年法是利用原子反应堆的快中子，先将矿物或岩石中的稳定态同位素 ^{39}K 活化为 ^{39}Ar。经中子活化后的样品，利用质谱分析方法，一次完成 ^{40}Ar、^{39}Ar、^{37}Ar 及 ^{36}Ar 等氩同位素的分析测量工作，经由 $^{40}Ar/^{39}Ar$ 比值推算出 $^{40}Ar^*/^{40}K$（$^{40}Ar^*$ 为放射性产生的氩的同位素）比值。然而在中子照射过程中，^{39}Ar 与 ^{39}K 含量的关系常数并非为定值，会随中子通量大小而改变，因此在实际操作过程中 $^{40}Ar/^{39}Ar$ 定年法系利用已知的K−Ar同位素年龄的矿物，即标准矿物与欲测年龄的样品一起放入原子反应堆中接受中子活化，求得一些与快中子通量有关的常数，进而计算得到样品同位素年代。

1.2 火山岩地球化学特征

1.2.1 火山岩地化数据测试方法

将采集的样品选送部分至中国科学院地质与地球物理研究所进行测试，数据见表2，测试项目为

图2 银–额盆地苏红图坳陷火山岩野外照片

A—块状玄武岩(41°12′067N,″104°12′929″ E);B—块状玄武岩(41°11′406 N,″104°13′333″E);C—杏仁状玄武安山岩(41°12′014 ″N,104°12′741″E);D—块状橄榄玄武岩(41°13′213 ″N,104°11′006″E);括号"( )"内经纬度表示火山岩的地理位置

Fig.2 Field photographs of volcanic rocks

A–Massive basalt(41°12′067N,″104°12′929″ E);B–Massive basalt(41°11′406 N,″104°13′333″E);C–Amygdaloidal basaltic andesite (41°12′014 ″N,104°12′741″E);D–Massive olivine basalt(41°13′213 ″N,104°11′006″E);The latitude and longitude in brackets denote the geographic location of volcanic rocks

常量元素、微量元素、Sr–Nd–Pb同位素,其中常量、微量元素测试各24件,同位素6件。

常量元素分析方法: 用0.6 g样品和6 g四硼酸锂制成的玻璃片在Shimadzu XRF–1500上测定氧化物的质量分数,精度优于2%~3%。

微量元素采用酸溶法: 样品溶液制备好后,在Element Ⅱ型ICP–MS上测试,按照GSR–1和GSR–2国家标准,元素质量分数大于10×10^{-6}的元素精度优于5%,小于10×10^{-6}的元素优于10%。

Sr、Nd同位素分析方法: 称取约100 mg全岩粉末样品,加入适量的^{87}Rb–^{84}Sr和^{149}Sm–^{150}Nd混合稀释剂和纯化的HF–$HClO_4$混合试剂后,在高温下完全溶解。Rb–Sr分离和纯化在装有5 mL AG50W–X12交换树脂(200~400目)的石英交换柱进行,Sm和Nd的分离和纯化是在石英交换柱用1.7 mL Teflon粉末为交换介质完成。采用^{146}Nd/^{144}Nd=0.7219和^{86}Sr/^{88}Sr=0.1194分别校正测得Nd和Sr同位素比值。Nd标样Jndi–1测定结果为^{143}Nd–^{144}Nd=0.512107,Sr标样NBS987测定结果为^{87}Sr–^{86}Sr = 0.710276。Rb–Sr和Sm–Nd的全流程本底分别为100 pg和50 pg左右。

Pb同位素的分析方法: 采用HF溶解样品,溶样后蒸干样品溶液,用6 mol/L HCl将氟化物样品转为氯化物,蒸干后,用0.6 mol/L HBr提取样品。在装有80 μL AGlx(100~200目)交换树脂的Teflon交换柱上,采用0.6 mol/L HBr和6 mol/L HCl流程分离纯化Pb样品。同位素比值测量采用德国Finnigan公司MAT262固体源质谱仪,^{147}Sm/^{144}Nd和^{87}Rb/^{86}Sr比值误差小于0.5%。

1.2.2 火山岩地球化学特征

苏红图组火山岩主、微量元素分析结果(表2)显示,SiO_2含量为47.58%~56.28%,为中基性火山

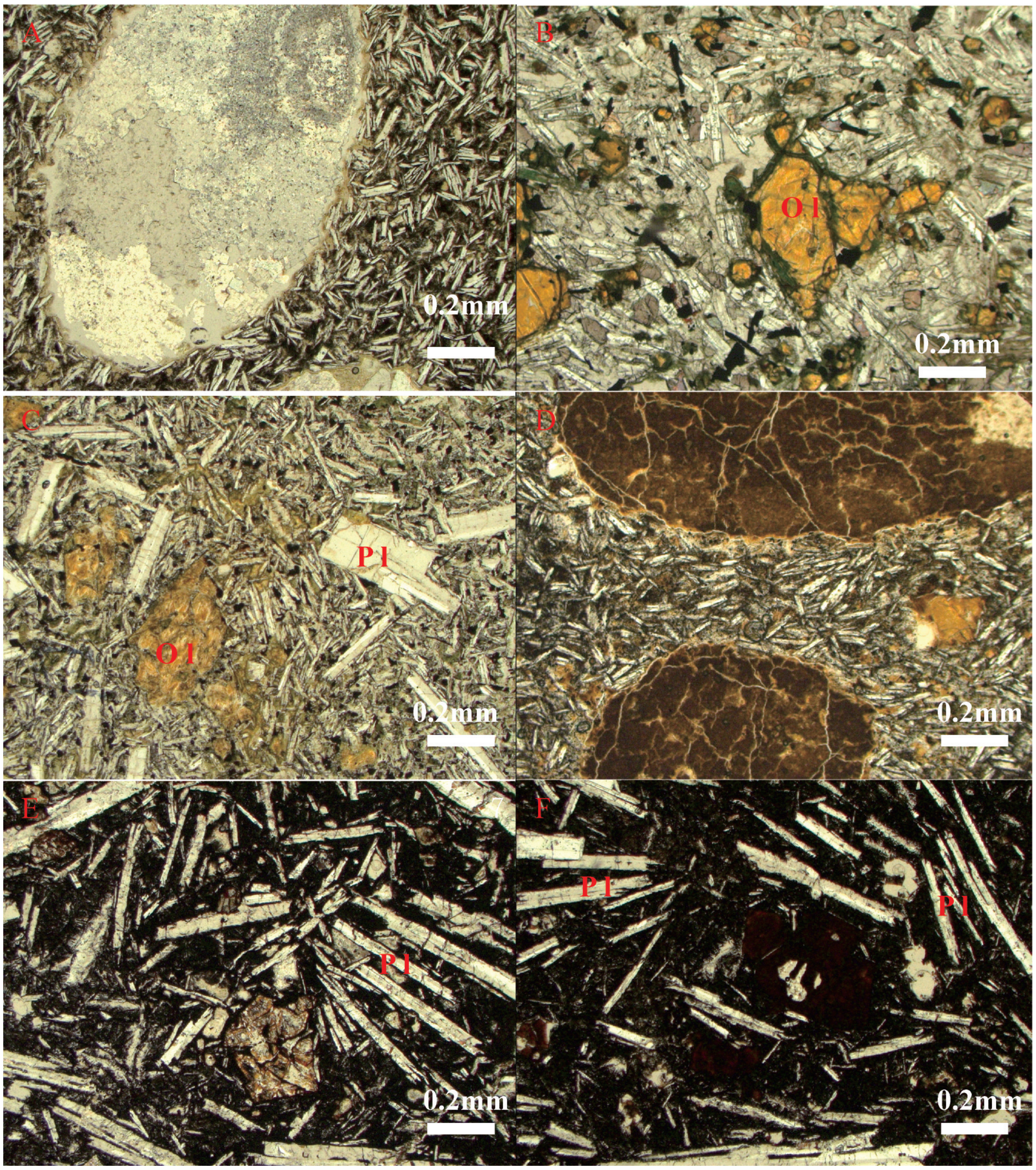

图3 银—额盆地苏红图坳陷火山岩镜下照片
A—杏仁状辉石安山岩;B—橄榄玄武岩;C—玄武岩;D—杏仁状辉石安山岩;E—杏仁状铁质玄武岩;
F—杏仁状橄榄铁质玄武岩;Pl—斜长石;Ol—橄榄石
Fig. 3 Microscope photographs of volcanic rocks
A–Amygdaloidal pyroxene andesite;B–Olivine basalt;C–Basalt;D–Amygdaloidal pyroxene andesite;E–Amygdaloidal iron basalt;
F–Amygdaloidal olivine iron basalt;Pl–Plagioclase;Ol–Olivine

岩,平均含量49.63%;里特曼指数为$4.7<\sigma<7.9$,平均值为6.3,属碱性系列火山岩;(K_2O+Na_2O)为4.95%~7.51%,平均含量为6.37%;在SiO_2−(K_2O+Na_2O)图解中24个样品均落在碱性玄武岩系列区域中(图5)。在SiO_2−K_2O图解中,绝大多数样品落在高钾玄武岩区域中(图6)。从微量元素蛛网图解(图7)中可以看出Nb、Ta元素具有富集的特点。

通过计算,苏红图火山岩的ε_{Nd}为−6.24~−3.08。$^{87}Sr/^{86}Sr$和$^{143}Nd/^{144}Nd$比值分别为0.705477~0.707098和0.512318~0.512480(表3)。$^{143}Nd/^{144}Nd$

表1 火山岩(Sht8、Sht11、Sht16、Sht18、Sht23、Sht28) $^{40}Ar/^{39}Ar$ 阶段升温分析结果

Table 1 Analytical results of $^{40}Ar/^{39}Ar$ stage warming

温度/ ℃	$^{40}Ar/^{39}Ar$	$^{37}Ar/^{39}Ar$	$^{36}Ar/^{39}Ar$	$^{40}Ar^*/^{39}Ar_k$	$^{40}Ar^*$/ %	$^{39}Ar_k$/ %	Age / Ma	± 2s /Ma
火山岩(Sht8)								
800	400.53596	1.89396	1.29445	18.204491	4.54	1.07	159.6	±83.3
850	600.56064	1.53985	1.91936	33.556077	5.58	3.56	284.1	±107.3
890	199.55504	1.25822	0.60574	20.681794	10.35	6.57	180.3	±36.2
930	42.46466	1.33096	0.10237	12.333764	29.01	13.84	109.7	± 6.6
960	33.16382	1.39697	0.06999	12.608255	37.97	11.62	112.0	± 4.5
990	33.04161	1.80096	0.07016	12.471141	37.69	6.09	110.8	± 4.6
1020	34.15268	1.44533	0.07368	12.509556	36.58	4.89	111.2	± 5.4
1050	31.62098	0.85513	0.06583	12.245327	38.70	4.01	108.9	± 5.0
1080	29.31229	0.70512	0.05814	12.193512	41.57	3.64	108.5	± 4.0
1110	24.09522	0.69613	0.03871	12.720275	52.76	5.07	113.0	± 2.8
1140	17.52755	1.26822	0.01754	12.458789	71.00	11.95	110.7	± 1.5
1170	19.37254	2.55239	0.02450	12.361393	63.67	7.50	109.9	± 2.1
1200	21.68269	4.25215	0.03216	12.563433	57.73	3.63	111.6	± 3.3
1260	21.02537	7.18903	0.03174	12.292286	58.11	4.41	109.3	± 2.9
1340	16.64307	6.99289	0.02219	10.704157	63.93	4.93	95.5	± 2.5
1450	17.09333	6.80533	0.01953	11.932095	69.40	7.23	106.2	± 1.8
火山岩(Sht11)								
800	701.20117	2.83541	2.37229	0.414464	0.06	0.34	3.6	±150.4
850	1347.6337	1.51256	4.54096	5.908866	0.44	1.83	50.7	±275.7
900	377.25698	1.54868	1.22754	14.659909	3.88	4.67	123.2	±70.7
950	94.59198	1.71983	0.26732	15.759120	16.64	13.26	132.2	±15.6
990	44.86243	1.25496	0.10511	13.915625	30.99	13.21	117.2	± 6.4
1030	33.75397	1.08670	0.06894	13.479338	39.90	10.35	113.6	± 4.4
1070	35.48988	0.81590	0.07659	12.932506	36.41	5.71	109.1	± 4.9
1110	27.21932	0.76648	0.04611	13.662610	50.16	6.75	115.1	± 3.3
1150	20.10580	1.47922	0.02323	13.376534	66.45	8.36	112.8	± 1.9
1180	21.19297	2.36783	0.02721	13.368360	62.95	5.71	112.7	± 2.7
1210	20.25695	2.63317	0.02429	13.319324	65.60	6.26	112.3	± 2.4
1260	19.66864	4.47057	0.02273	13.358679	67.66	10.48	112.6	± 1.9
1330	21.43974	9.43589	0.03002	13.427904	62.13	4.98	113.2	± 2.7
1450	20.24739	7.92726	0.02506	13.563974	66.54	8.11	114.3	± 2.1
火山岩（Sht16）								
800	40.90162	0.46527	0.13673	0.534630	1.31	2.08	4.7	±150.4
850	90.03898	0.97592	0.28733	5.214394	5.79	4.43	45.6	±275.7
900	45.48567	1.43442	0.11843	10.617135	23.31	6.73	91.7	±70.7
940	17.64187	0.59178	0.01755	12.509980	70.88	10.28	107.5	±15.6
980	16.97458	0.36660	0.01484	12.620800	74.33	9.48	108.4	± 6.4
1020	17.96807	0.34655	0.01868	12.478521	69.43	5.35	107.3	± 4.4
1050	17.62515	0.38095	0.01844	12.208998	69.25	6.23	105.0	± 4.9
1080	16.99371	0.40724	0.01694	12.023626	70.73	6.46	103.5	± 3.3
1110	16.83544	0.46998	0.01576	12.221395	72.56	7.12	105.1	± 1.9
1140	17.32462	0.49255	0.01683	12.394906	71.51	8.02	106.6	± 2.7
1170	18.15213	0.66033	0.01937	12.486624	68.75	7.63	107.3	± 2.4
1200	18.69208	1.03487	0.02142	12.456461	66.58	6.43	107.1	± 1.9
1250	18.87149	1.61694	0.02162	12.627883	66.82	9.50	108.5	± 2.7
1330	22.92370	2.06242	0.03613	12.433196	54.14	4.52	106.9	± 2.1
1450	22.39469	1.88448	0.03420	12.459035	55.54	5.74	107.1	± 2.3
火山岩（Sht18）								
800	78.74380	0.56554	0.26173	1.448856	1.84	1.97	12.9	±18.2
850	189.24489	0.96147	0.62531	4.544667	2.40	4.38	40.3	±40.6
900	94.08039	1.18663	0.28533	9.870298	10.48	7.77	86.3	±17.8
940	21.27121	0.43903	0.03040	12.328428	57.94	9.48	107.2	± 2.0
980	20.05984	0.38474	0.02585	12.455932	62.07	8.75	108.3	± 2.0
1020	21.02690	0.36767	0.03005	12.179294	57.90	6.40	105.9	± 2.1
1050	21.58730	0.37745	0.03226	12.088074	55.98	6.96	105.2	± 2.3
1080	23.09013	0.48025	0.03766	12.002888	51.96	9.80	104.5	± 2.5
1110	24.75671	0.56895	0.04324	12.029227	48.57	7.43	104.7	± 2.8
1140	25.41226	0.60758	0.04502	12.163771	47.84	7.48	105.8	± 3.0
1170	27.03045	0.67962	0.04993	12.335917	45.61	8.17	107.3	± 3.2
1200	25.33075	0.86710	0.04448	12.263561	48.38	6.83	106.7	± 3.4
1250	26.59450	1.34128	0.04871	12.319973	46.27	6.23	107.1	± 3.3
1330	29.33296	1.72995	0.05849	12.205260	41.55	3.00	106.2	± 4.0
1450	28.11178	1.56163	0.05306	12.571883	44.66	5.36	109.3	± 3.5
火山岩（Sh23）								
800	243.87498	1.07126	0.79933	7.763698	3.18	1.08	68.7	±54.4
850	452.17901	0.85577	1.49424	10.707317	2.37	2.97	94.1	±90.7
900	123.49801	0.79431	0.38590	9.532681	7.71	5.21	84.0	±23.7
940	30.29007	0.88810	0.06454	11.297737	37.27	10.89	99.2	± 4.4
980	26.58034	0.85804	0.05034	11.781364	44.29	10.92	103.3	± 3.4
1020	32.87398	0.89845	0.07028	12.185219	37.04	7.03	106.7	± 4.6
1050	33.23477	0.66023	0.07069	12.405373	37.31	5.72	108.6	± 4.7
1080	20.65185	0.50446	0.02798	12.429463	60.16	6.00	108.8	± 2.0
1110	17.31100	0.67712	0.01705	12.332348	71.20	6.45	108.0	± 1.7
1140	17.65415	0.89421	0.01825	12.340914	69.85	5.85	108.1	± 1.7
1170	19.93714	0.90509	0.02608	12.312473	61.71	7.45	107.8	± 1.9
1200	17.47566	1.38969	0.01738	12.465453	71.25	11.03	109.1	± 1.4
1250	16.89189	2.52097	0.01591	12.416105	73.35	9.15	108.7	± 1.4
1330	16.93102	5.20982	0.01683	12.428147	73.08	4.81	108.8	± 1.7
1450	17.41517	8.93531	0.01960	12.429052	70.83	5.44	108.8	± 1.6

续表1

温度/ ℃	$^{40}Ar/^{39}Ar$	$^{37}Ar/^{39}Ar$	$^{36}Ar/^{39}Ar$	$^{40}Ar^*/^{39}Ar_k$	$^{40}Ar^*$/ %	$^{39}Ar_k$/ %	Age / Ma	± 2s /Ma
火山岩（Sht28）								
800	296.49593	0.88497	0.95605	14.063408	4.74	2.07	123.4	±74.2
880	249.96868	0.61497	0.76178	24.925178	9.97	8.72	213.3	±47.0
960	24.55579	0.65110	0.04308	11.882813	48.36	29.39	104.8	± 3.0
990	25.76912	0.71244	0.04589	12.271538	47.59	7.92	108.2	± 2.9
1020	31.25041	0.63736	0.06364	12.502820	39.99	4.21	110.1	± 4.5
1050	30.65379	0.48972	0.06100	12.672812	41.32	3.22	111.6	± 4.6
1100	25.25518	0.45594	0.04399	12.296685	48.67	4.20	108.4	± 3.3
1150	21.61958	0.56800	0.03143	12.381785	57.24	5.04	109.1	± 2.5
1200	20.56691	0.75113	0.02708	12.632402	61.38	9.43	111.2	± 2.0
1230	15.97513	1.11264	0.01219	12.472792	78.00	6.89	109.9	± 1.7
1260	15.32703	1.94431	0.01041	12.426233	80.94	7.74	109.5	± 1.4
1290	15.40786	2.75785	0.01136	12.298386	79.63	4.05	108.4	± 1.9
1340	15.38935	7.21215	0.01230	12.404024	80.11	4.97	109.3	± 1.6
1390	19.09551	12.69582	0.02723	12.190053	63.15	1.73	107.5	± 4.5
1450	26.42477	8.59044	0.05675	10.412478	39.12	0.43	92.2	±10.5

注:由中国科学院地质与地球物理研究所测试。

比值均小于未分异球粒陨石地幔值0.512638。在$^{87}Sr/^{86}Sr$、$^{143}Nd/^{144}Nd$及ε_{Nd}相关性图解上(图8),火山岩的Nd、Sr同位素组成靠近第一类富集地幔(EMI)端元,并有向EMⅡ延伸的趋势,显示火山岩源区主要受EMI控制,并受EMⅡ的微弱影响。通过火山岩$^{206}Pb/^{204}Pb$与$^{207}Pb/^{204}Pb$、$^{206}Pb/^{204}Pb$与$^{208}Pb/^{204}Pb$关系图解(图9)也可以看出,该区火山岩主要受EMI源区的影响。

2　苏红图火山岩形成及动力学机制

2.1 苏红图火山岩形成机制

火山岩样品中Nb、Ta元素具有富集的特点,显示出了具有洋岛玄武岩(OIB)特征,说明了苏红图火山岩岩浆主要来自于对流的软流圈地幔;而从同位素特点来看,该区6个火山岩ε_{Nd}均小于0,为−6.24~−3.08,很显然岩浆源区具有富集的特征,且在$^{87}Sr/^{86}Sr$、$^{143}Nd/^{144}Nd$及ε_{Nd}相关性图解上,火山岩的Nd、Sr同位素组成靠近第一类富集地幔(EMI)端元,并有向EMⅡ延伸的趋势,显示本区火山岩的源区受EMI影响很大,受EMⅡ的微弱影响,对该区火山岩$^{206}Pb/^{204}Pb$与$^{207}Pb/^{204}Pb$、$^{206}Pb/^{204}Pb$与$^{208}Pb/^{204}Pb$关系图解,也可以看出,该区火山岩主要受EMI源区的影响。

从图10中可以看出,随着ε_{Nd}的减少,Zr、P_2O_5、Rb、Sr、Ba及Nb逐渐富集,暗示着苏红图火山岩没有经历明显的地壳物质混染。而Na_2O、CaO等主量元素随着ε_{Nd}(ε_{Nd}=−6.24~−3.08)的增加而增加,是因为随着部分熔融程度增加,地幔中的角闪石、金红石和金云母开始部分熔融,富集了Na和Ca元素。此外,如果火山岩岩浆被上地壳物质混染,$^{87}Sr/^{86}Sr$比值应该更大些,变化范围更宽些。苏红图火山岩$^{87}Sr/^{86}Sr$值远小于现今大陆地壳$^{87}Sr/^{86}Sr$比值(表3中平均为0.719),也可以说明它们没有受到明显的地壳物质混染,此外,低Rb/Ba、Rb/Sr值和高Ti/Y值排除了岩浆被地壳混染的可能。

从La/Sm−La图解(图11)显示苏红图火山岩岩浆既有部分熔融特征,又带有分离结晶的特征。因此,苏红图火山岩可能为平衡部分熔融及随后的分离结晶共同作用的产物。

2.2 苏红图火山岩喷发动力学机制

目前为止,人们对西伯利亚、华北和塔里木等稳定块体之间的碰撞拼合已有了较为一致的认识[4,27−31]。Zhao Xixi等[27]根据古地磁研究结果,提出西伯利亚板块、内蒙古褶皱带和华北板块的碰撞拼合最后结束时间为晚侏罗世;任收麦等[4]通过对苏红图火山岩古地磁研究,提出在早白垩世,西伯利亚板块、内蒙古褶皱带和华北块体在动力学上已成为整体;研究认为苏红图坳陷火山岩属于钾质碱性玄武岩,而钾质碱性玄武岩通常只形成于大陆环境[32],通过对火山岩微量元素分析也得到相同结论(图12~13)。银—额盆地内的地震资料表明[33],当时盆地沉降和沉积充填受张性断裂构造控制,且岩浆活动并不仅仅局限于银—额盆地,在其周缘、南蒙古地区、甚至在整个中亚地区都普遍出现,说明了早白垩世的岩石圈在较大范围内处于一种拉伸状态[33],岩石圈厚度为90 km左右[34]。

所以,由于西伯利亚板块、内蒙古褶皱带和华北地块在晚侏罗世碰撞拼合,导致华北克拉通西北部苏红图坳陷下伏岩石圈减薄,随着岩石圈地幔的

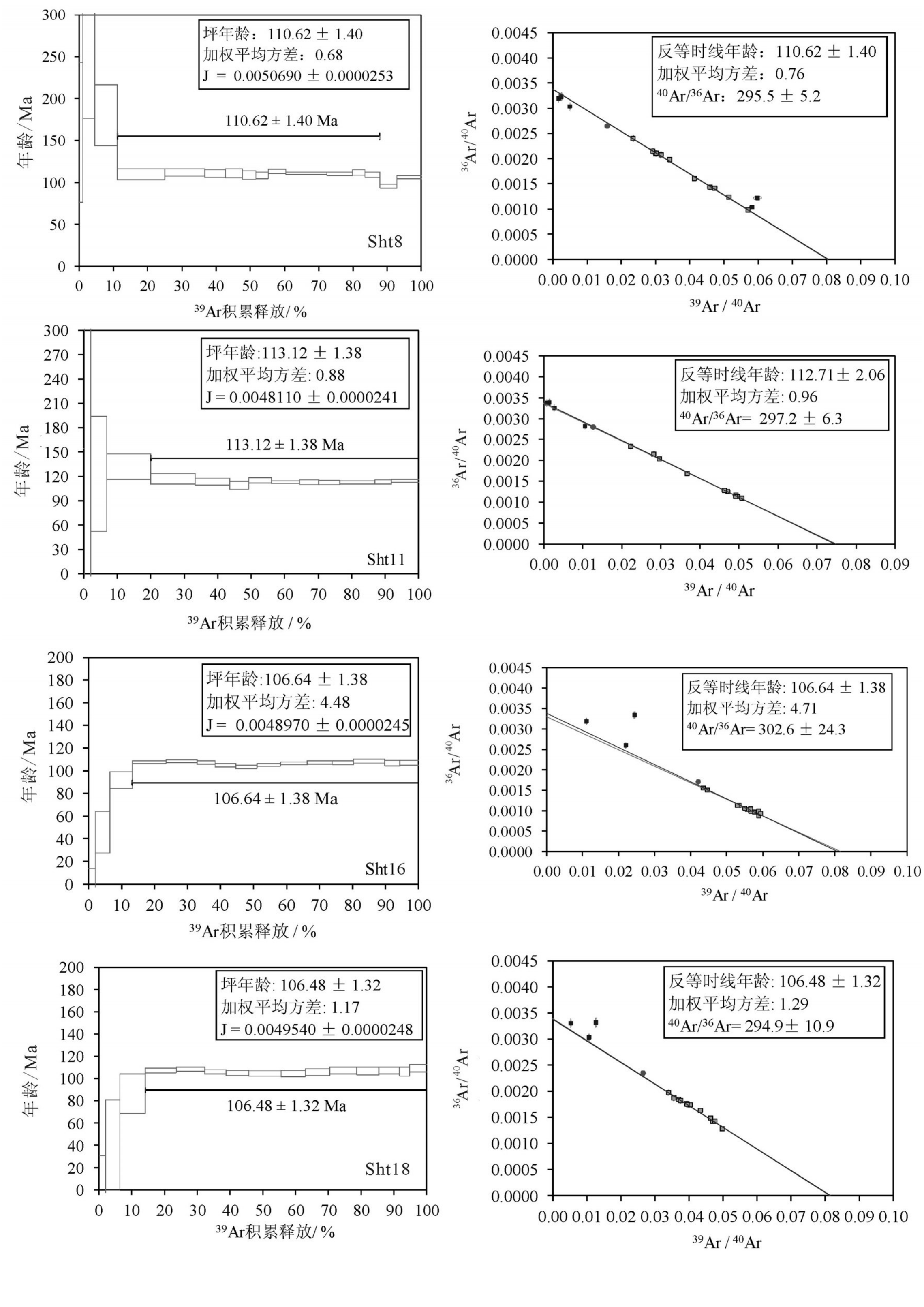

坪年龄：110.62 ± 1.40
加权平均方差：0.68
J = 0.0050690 ± 0.0000253
110.62 ± 1.40 Ma
Sht8
年龄/Ma
39Ar积累释放/%
反等时线年龄：110.62 ± 1.40
加权平均方差：0.76
40Ar/36Ar：295.5 ± 5.2
36Ar/40Ar
39Ar / 40Ar
坪年龄:113.12 ± 1.38
加权平均方差: 0.88
J = 0.0048110 ± 0.0000241
113.12 ± 1.38 Ma
Sht11
年龄/Ma
39Ar积累释放/%
反等时线年龄: 112.71 ± 2.06
加权平均方差: 0.96
40Ar/36Ar= 297.2 ± 6.3
36Ar/40Ar
39Ar / 40Ar
坪年龄:106.64 ± 1.38
加权平均方差: 4.48
J = 0.0048970 ± 0.0000245
106.64 ± 1.38 Ma
Sht16
年龄/Ma
39Ar积累释放/%
反等时线年龄: 106.64 ± 1.38
加权平均方差: 4.71
40Ar/36Ar= 302.6 ± 24.3
36Ar/40Ar
39Ar / 40Ar
坪年龄: 106.48 ± 1.32
加权平均方差: 1.17
J = 0.0049540 ± 0.0000248
106.48 ± 1.32 Ma
Sht18
年龄/Ma
39Ar积累释放/%
反等时线年龄: 106.48 ± 1.32
加权平均方差: 1.29
40Ar/36Ar= 294.9 ± 10.9
36Ar/40Ar
39Ar / 40Ar

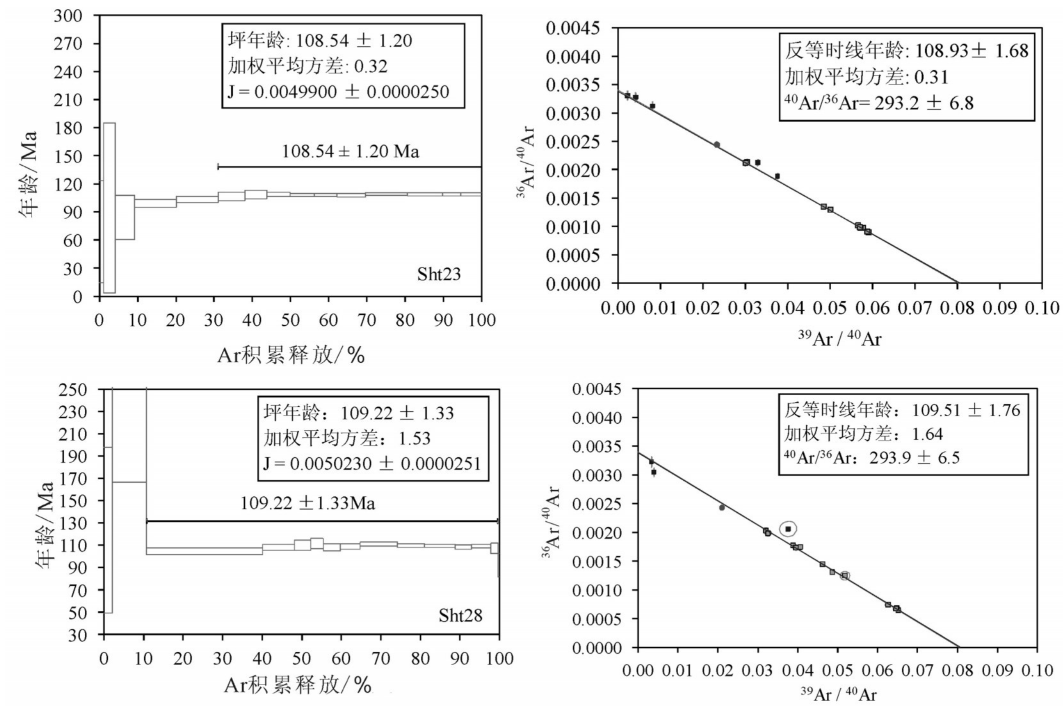

图4 火山岩(Sht8、Sht11、Sht16、Sht18、Sht23、Sht28)坪年龄与反等时线年龄
Fig.4 Plateau age and reverse isochron age of Suhongtu volcanic rocks

减薄,在早白垩世(105~113 Ma)该区下伏软流圈地幔岩浆上涌,在上涌的过程中没有经历地壳物质的明显混染,经平衡部分熔融及随后的分离结晶共同作用形成陆内苏红图高钾玄武岩。

3 克拉通破坏时间与范围的探讨

华北克拉通破坏时间与范围是克拉通破坏研究的重要科学问题。许多学者利用华北克拉通破坏在地壳浅部产生的响应对这些问题展开了一系列研究,但并没有达成统一共识。文章前面部分对位于华北克拉通西北缘的苏红图火山岩年代学与地球化学进行了研究,下面主要针对前人对华北克拉通研究成果,结合本文作者在苏红图火山岩方面所做的一些工作,对华北克拉通在破坏时间与范围上进行一些探讨。

岩浆活动是华北克拉通破坏在地壳浅部产生的重要响应之一。华北地区岩浆活动从晚古生代到新生代均有发育(图14)。华北地区最早的岩浆活动出现在华北北缘的内蒙古隆起(图14-a),为一套钙碱性、I型花岗岩,年龄主要分布在324~300 Ma[35]。晚石炭世岩浆活动说明了当时克拉通边缘岩石圈结构和热状态发生了改变,因此无论是何种岩浆动力学机制,正是自晚石炭世开始华北克拉通周边发生了多次构造拼贴和相关岩浆活动,拉开了华北岩石圈破坏的序幕。所以,由此认为华北克拉通有可能是从晚石炭世开始发生破坏的[15,35]。

晚三叠世岩浆作用的分布较为局限,主要分布在苏鲁超高压变质带及其北延部分(图14-b)。根据Chen et al.[36]和Xie et al.[37]的研究,发育在甲子山的晚三叠世正长岩是由于扬子板块向华北板块俯冲过程中发生板片断离,软流圈地幔沿板片窗上涌导致上覆华北岩石圈地幔发生熔融所致。研究显示在徐淮弧形构造区内早侏罗世(191 Ma)同造山侵入岩中发现的高压榴辉岩包体[38]及在徐淮弧形构造带中发育的早侏罗世和早白垩世侵入杂岩体中发现了含220 Ma的榴辉岩捕虏体[39],与大别—苏鲁造山带超高压变质作用时间一致。这一结果暗示扬子地块与华北板块碰撞导致了华北克拉通的破坏,即碰撞导致了华北下地壳的加厚,形成了大量榴辉岩,继而发生拆沉作用[19,40]。所以,在晚三叠世,克拉通边缘的岩石圈结构和热状态发生了改变。

华北地区大约从中侏罗世开始出现较大范围

表2 银—额盆地苏红图坳陷火山岩岩石地球化学分析结果

Table 2 Analytical results of volcanic rocks

	Sht-04	Sht-05	Sht-06	Sht-07	Sht-08	Sht-09	Sht-10	Sht-11	Sht-12	Sht-13	Sht-14	Sht-15
SiO_2 / %	49.96	48.13	47.90	49.40	47.80	48.60	47.85	47.90	49.03	47.58	49.45	52.02
TiO_2	2.03	1.73	1.77	2.04	1.79	1.94	1.76	1.75	2.01	1.69	2.13	1.98
Al_2O_3	17.94	15.84	15.97	16.55	15.69	16.34	15.66	15.54	16.16	15.75	16.80	17.74
TFe_2O_3	7.17	11.10	10.79	9.82	11.38	10.74	11.28	11.32	10.31	10.99	9.84	7.60
MnO	0.07	0.16	0.13	0.13	0.15	0.13	0.15	0.16	0.14	0.16	0.17	0.09
MgO	4.63	7.31	6.55	5.38	7.06	5.93	7.61	7.82	5.84	7.60	5.02	4.56
CaO	6.33	6.20	6.85	6.19	6.88	7.61	7.33	6.52	6.66	6.41	7.34	4.85
Na_2O	3.75	5.29	4.39	5.15	4.09	3.34	3.41	4.51	4.70	4.59	3.62	4.03
K_2O	3.02	1.07	1.03	1.77	1.47	1.77	1.55	1.17	1.86	1.16	2.18	2.99
P_2O_5	1.05	0.43	0.44	0.59	0.43	0.48	0.43	0.44	0.57	0.43	0.60	0.85
LOI	3.88	3.02	4.24	2.96	3.16	3.10	3.14	3.06	2.86	3.42	2.26	2.70
Total	99.83	100.26	100.06	99.98	99.91	99.98	100.16	100.18	100.14	99.77	99.42	99.41
Li / 10^{-6}	56.03	22.40	31.40	21.82	33.15	30.86	27.51	26.35	20.58	29.70	41.19	41.01
Be	0.97	1.13	1.15	1.57	1.11	1.27	1.10	1.11	1.51	1.12	1.10	1.10
Sc	16.82	26.27	26.66	24.72	26.00	26.54	26.70	26.96	24.70	26.41	25.00	18.12
V	111.10	169.61	167.80	156.65	170.66	170.98	172.59	171.010	157.68	168.85	165.84	116.66
Cr	49.17	237.14	221.13	181.90	234.46	222.06	274.12	230.59	188.94	233.57	178.54	69.22
Co	25.47	41.56	39.49	32.76	41.20	37.61	40.86	43.52	35.09	42.20	34.54	25.35
Ni	42.07	112.34	109.12	78.92	114.76	102.33	114.31	119.61	93.34	111.24	96.49	33.23
Cu	23.64	42.28	46.19	42.76	48.22	50.18	44.57	38.77	37.85	44.72	57.75	33.29
Zn	121.00	98.73	95.83	97.52	98.33	99.42	95.31	99.44	95.39	100.12	121.60	149.72
Ga	23.29	18.60	18.71	19.28	18.98	19.99	17.76	17.84	19.21	18.44	20.21	23.81
Rb	26.86	7.60	6.87	45.63	25.27	31.09	25.23	9.54	47.53	10.72	37.72	33.77
Sr	827.17	338.17	406.24	473.09	447.89	549.36	473.00	324.93	509.25	314.08	555.06	747.77
Y	41.13	25.97	25.78	30.72	26.25	28.17	25.96	27.33	30.96	25.89	30.99	36.64
Zr	331.88	172.19	172.11	236.21	172.73	190.96	170.12	173.99	224.93	165.93	217.00	367.20
Nb	57.28	29.24	29.22	42.17	29.40	32.34	29.50	30.30	41.94	28.92	40.05	56.91
Cs	0.29	8.59	6.35	8.36	5.54	1.26	1.99	7.23	6.21	7.21	0.39	0.15
Ba	1296.51	543.63	446.16	731.17	482.08	625.00	519.31	542.94	708.23	514.73	684.56	1124.50
La	62.32	23.29	23.10	33.46	23.58	26.11	22.98	24.27	33.45	22.75	32.89	56.15
Ce	126.34	45.43	45.30	64.43	45.97	50.51	45.46	47.40	64.27	44.17	64.04	115.74
Pr	15.99	5.88	5.68	8.18	5.90	6.55	5.88	6.22	7.96	5.66	8.10	14.15
Nd	62.94	23.77	23.04	33.42	24.29	26.14	23.03	24.44	32.00	23.00	33.76	54.55
Sm	11.21	5.22	5.06	6.57	5.40	5.67	4.91	5.39	6.52	5.05	6.76	10.37
Eu	2.71	1.75	1.67	2.03	1.74	1.88	1.73	1.73	2.15	1.69	2.18	2.60
Gd	10.40	5.35	5.23	6.55	5.32	5.78	4.94	5.02	5.97	4.93	6.29	9.35
Tb	1.53	0.88	0.84	1.02	0.86	0.94	0.81	0.82	0.97	0.81	0.99	1.34
Dy	8.37	5.25	5.04	6.07	5.29	5.57	4.94	5.27	5.90	4.79	5.86	7.13
Ho	1.62	1.05	1.03	1.25	1.06	1.17	1.02	1.06	1.18	0.97	1.18	1.42
Er	4.19	2.84	2.81	3.26	2.88	3.07	2.74	2.83	3.12	2.63	3.10	3.69
Tm	0.59	0.40	0.40	0.47	0.42	0.44	0.39	0.42	0.47	0.39	0.46	0.53
Yb	3.65	2.51	2.50	3.02	2.58	2.75	2.50	2.61	3.02	2.47	2.85	3.32
Lu	0.54	0.38	0.38	0.46	0.39	0.41	0.38	0.38	0.46	0.37	0.43	0.50
Hf	8.99	4.27	4.23	5.78	4.28	4.78	4.21	4.33	5.47	3.99	5.38	8.83
Ta	3.51	1.86	1.85	2.72	1.90	2.11	1.82	1.91	2.55	1.81	2.53	3.58
Tl	0.13	0.05	0.04	0.07	0.06	0.07	0.06	0.05	0.07	0.05	0.06	0.11
Pb	10.12	3.56	4.33	6.00	3.29	3.44	3.08	3.10	4.17	3.07	4.46	7.32
Bi	0.06	0.01	0.01	0.01	0.01	0.01	0.01	0.01	0.01	0.01	0.02	0.02
Th	5.45	2.34	2.31	3.59	2.40	2.66	2.18	2.34	3.48	2.20	3.26	5.49
U	2.23	0.57	0.59	0.86	0.54	0.62	0.53	0.60	0.91	0.58	0.47	1.02
REE	312.39	123.98	122.08	170.18	125.68	136.99	121.69	127.85	167.42	119.68	168.88	280.82
LREE	281.51	105.34	103.85	148.09	106.88	116.86	103.98	109.46	146.35	102.32	147.73	253.55
HREE	30.89	18.65	18.23	22.09	18.80	20.13	17.71	18.39	21.07	17.36	21.14	27.27
LREE/HREE	9.11	5.65	5.70	6.70	5.69	5.81	5.87	5.95	6.94	5.89	6.99	9.30
δCe	0.94	0.91	0.93	0.91	0.91	0.91	0.92	0.91	0.92	0.91	0.92	0.96
δEu	0.75	1.00	0.98	0.94	0.98	1.00	1.06	1.00	1.03	1.02	1.01	0.79

续表2

	Sht-16	Sht-17	Sht-18	Sht-19	Sht-20	Sht-21	Sht-22	Sht-23	Sht-25	Sht-26	Sht-27	Sht-28
SiO_2 / %	54.63	51.14	56.28	49.78	51.51	48.77	48.68	49.00	48.88	49.24	48.82	48.88
TiO_2	1.83	2.09	1.89	2.12	2.00	2.12	2.04	2.04	2.01	2.04	1.95	2.02
Al_2O_3	15.44	16.67	14.67	16.67	15.69	16.93	16.21	16.42	16.59	16.48	16.33	16.31
TFe_2O_3	8.88	9.05	10.96	9.42	9.34	10.33	10.42	9.24	9.08	9.19	9.38	9.30
MnO	0.10	0.12	0.06	0.13	0.15	0.19	0.17	0.14	0.13	0.14	0.14	0.14
MgO	0.51	0.94	0.78	4.94	1.48	5.64	6.29	5.95	6.03	5.91	6.49	6.31
CaO	7.34	8.36	5.52	6.77	7.76	6.32	6.85	6.36	6.62	6.11	6.87	6.57
Na_2O	3.88	4.48	4.00	4.23	4.13	3.62	3.53	5.19	5.03	5.39	4.68	4.87
K_2O	2.90	3.03	2.95	2.28	3.09	2.24	2.08	1.87	2.00	1.89	1.84	1.74
P_2O_5	0.72	0.81	0.72	0.60	0.72	0.60	0.58	0.61	0.60	0.62	0.59	0.58
LOI	3.18	3.59	2.04	2.66	4.00	2.70	2.94	2.68	2.38	2.82	2.60	2.74
Total	99.41	100.29	99.89	99.61	99.88	99.45	99.80	99.50	99.35	99.84	99.69	99.46
Li / 10^{-6}	51.27	33.06	43.04	37.02	30.72	55.37	52.80	22.98	11.90	25.98	29.19	22.17
Be	1.56	1.49	1.87	1.77	3.18	1.20	1.15	1.89	1.65	1.68	1.58	1.65
Sc	16.89	18.52	15.04	24.81	18.15	25.36	24.03	22.19	23.00	21.79	22.99	23.24
V	110.17	127.71	101.98	168.64	134.03	172.95	156.32	141.32	142.06	134.99	149.07	148.43
Cr	137.28	133.09	124.20	188.84	128.91	190.88	177.89	130.34	153.00	125.47	225.73	149.68
Co	10.38	16.14	13.62	34.50	15.18	38.26	34.86	30.77	30.98	30.07	33.68	32.53
Ni	15.93	33.58	27.84	85.25	27.69	92.24	93.17	78.89	79.88	77.56	88.85	85.09
Cu	22.43	47.30	26.60	41.63	33.17	37.41	27.83	32.47	31.57	32.43	30.84	31.67
Zn	48.99	62.79	50.23	108.78	63.35	130.00	117.27	98.94	85.21	85.94	86.53	89.86
Ga	18.49	19.77	18.34	18.89	19.42	20.91	19.21	19.04	19.01	19.22	18.61	18.65
Rb	58.56	59.02	58.25	45.28	64.20	40.99	36.13	12.03	18.74	13.73	13.00	15.88
Sr	643.49	634.63	642.72	509.84	609.82	542.11	489.81	554.08	600.25	539.63	564.15	574.73
Y	29.67	30.21	28.17	29.53	28.75	29.33	28.53	26.94	27.71	27.95	26.40	27.65
Zr	262.42	264.97	262.25	222.85	282.83	211.46	205.21	223.30	229.76	233.31	223.98	229.86
Nb	46.63	49.15	47.02	43.77	47.30	40.90	38.31	48.04	48.98	50.79	47.41	49.40
Cs	1.57	1.26	3.19	14.48	1.81	0.51	1.46	1.86	1.26	2.12	1.52	1.62
Ba	1659.75	816.17	782.62	877.45	1029.91	706.57	605.90	810.74	809.16	792.00	818.67	846.99
La	37.04	40.77	38.03	33.07	37.33	32.15	31.53	32.43	34.10	34.66	33.41	34.20
Ce	73.69	80.76	75.49	66.92	74.31	61.69	61.16	62.00	64.78	65.16	62.90	63.77
Pr	9.47	10.56	9.73	8.41	9.73	8.24	7.79	7.75	7.93	8.14	7.97	8.07
Nd	37.21	40.36	38.48	33.88	37.84	32.39	30.45	30.27	31.32	30.95	30.60	31.63
Sm	6.95	7.51	7.25	6.82	7.48	6.82	6.29	6.01	6.50	6.41	6.19	6.27
Eu	2.09	2.27	2.04	2.12	2.13	2.18	2.11	2.07	2.12	2.16	1.98	2.00
Gd	6.84	7.20	6.88	6.57	7.40	6.88	5.77	5.74	5.63	5.93	5.64	5.74
Tb	0.99	1.06	0.97	0.99	1.03	1.01	0.89	0.86	0.91	0.94	0.91	0.89
Dy	5.60	5.98	5.53	5.79	5.57	5.78	5.42	5.09	5.29	5.51	5.11	5.33
Ho	1.13	1.15	1.13	1.16	1.09	1.16	1.08	0.99	1.04	1.08	1.01	1.04
Er	3.04	3.07	2.99	3.10	2.98	3.12	2.88	2.64	2.65	2.80	2.69	2.79
Tm	0.44	0.45	0.44	0.46	0.44	0.46	0.42	0.38	0.39	0.40	0.39	0.40
Yb	2.90	2.95	2.77	2.95	2.82	2.91	2.51	2.41	2.46	2.48	2.49	2.54
Lu	0.44	0.44	0.42	0.45	0.43	0.44	0.37	0.36	0.37	0.39	0.38	0.39
Hf	6.04	6.23	6.18	5.37	5.78	5.28	5.06	5.62	5.61	5.85	5.48	5.87
Ta	2.77	2.91	2.87	2.67	2.69	2.53	2.36	3.04	3.09	3.12	3.02	3.23
Tl	0.140	0.12	0.17	0.09	0.14	0.06	0.05	0.045	0.07	0.05	0.15	0.06
Pb	7.000	6.15	8.29	4.34	7.12	4.08	3.89	3.94	4.15	4.12	4.17	4.20
Bi	0.014	0.01	0.02	0.01	0.03	0.02	0.01	0.011	0.01	0.01	0.01	0.01
Th	3.710	3.81	3.84	3.87	3.55	3.30	2.94	3.35	3.49	3.61	3.72	3.65
U	0.98	1.44	1.13	0.93	2.50	0.43	0.53	0.94	1.00	0.96	0.97	1.03
REE	187.81	204.53	192.13	172.68	190.57	165.22	158.68	158.99	165.48	167.01	161.65	165.05
LREE	166.43	182.22	171.02	151.21	168.81	143.47	139.33	140.52	146.75	147.48	143.03	145.93
HREE	21.38	22.30	21.12	21.46	21.76	21.76	19.35	18.48	18.73	19.53	18.62	19.12
LREE/HREE	7.78	8.17	8.10	7.05	7.76	6.59	7.20	7.61	7.83	7.55	7.68	7.63
δCe	0.93	0.92	0.92	0.94	0.92	0.89	0.91	0.91	0.92	0.90	0.90	0.89
δEu	0.92	0.93	0.87	0.96	0.87	0.96	1.05	1.06	1.05	1.06	1.00	1.00

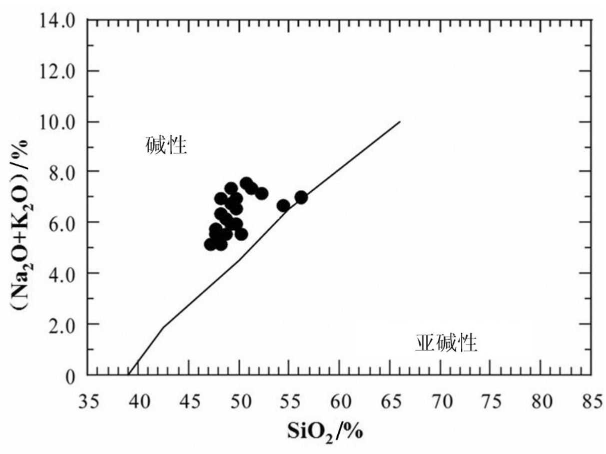

图5 SiO_2−(K_2O+Na_2O)图解
Fig.5 SiO_2−(K_2O+Na_2O) diagram

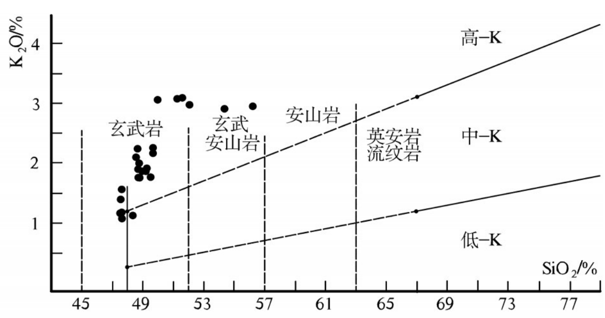

图6 SiO_2−K_2O图解
Fig. 6 SiO_2−K_2O diagram

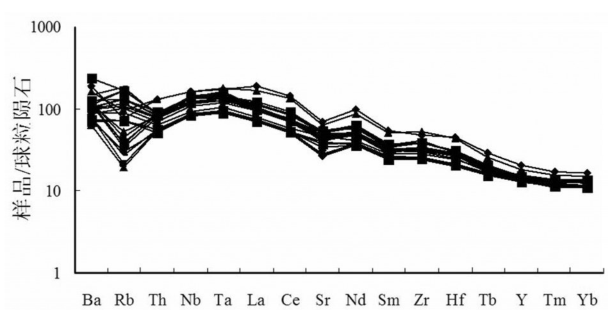

图7 苏红图火山岩微量元素/球粒陨石标准化模式图
Fig. 7 Chondrite−normalized trace element diagram

的岩浆活动(图14−C),其活动时期主要在190~155 Ma[22,41,42]。Gao et al.[20]通过对辽西地区中生代高镁adakite研究,结合该岩石高Ni和Cr含量及其在矿物中的分布特征,认为这些岩石是拆沉进入地幔的

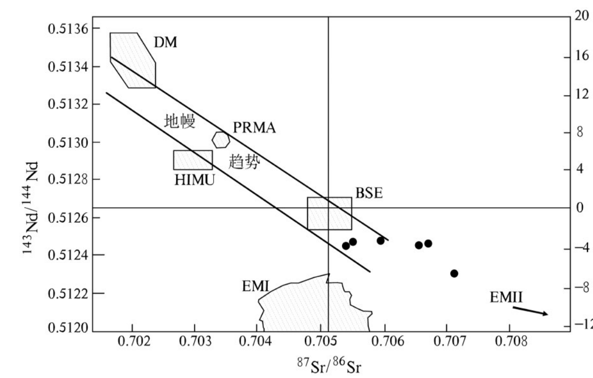

图8 $^{87}Sr/^{86}Sr$、$^{143}Nd/^{144}Nd$及ε_{Nd}关系图解[25]
DM—亏损地幔;BSE—全硅酸盐地球;EM I、EM II—富集地幔I、II;HIMU—具有高U / Pb比值的地幔;PREMA—普通地幔
Fig. 8 Diagram showing relationships between $^{87}Sr/^{86}Sr$, $^{143}Nd/^{144}Nd$ and ε_{Nd}[25]
DM−Depleted mantle;BSE−Whole silicate earth;EM I, EM II−Type I and II enriched mantle;HIMU−Range of high U/Pb ratio mantle;PREMA−Ordinary mantle

地壳岩石部分熔融而成,从而暗示华北克拉通的破坏发生在中侏罗世以后。Charles et al.[43]认为晚侏罗世时华北克拉通东部南、北缘局部开始了伸展活动,但是在其内部还很少发育岩浆活动与伸展构造,反映了在该时期华北克拉通东部岩石圈的改造只发生在其南、北缘[24]。在克拉通东部南缘胶北地区与合肥盆地北缘发现了晚侏罗世的玲珑岩基和荆山—涂山花岗岩体,研究表明这些晚侏罗世岩浆活动是发生在岩石圈减薄的环境中[44−46]。

在晚侏罗世—早白垩世时期,岩浆活动的范围和强度达到了顶峰,除了分布在燕山、太行山和苏鲁大别带外,也出现在华北地台腹地及郯庐断裂两侧,且岩浆活动呈现出由克拉通边缘向克拉通腹地迁移的趋势(图14−d)[47]。此外,在克拉通西北缘的苏红图坳陷在早白垩世时期也发生了强烈的岩浆活动。克拉通破坏在地壳浅部响应除了岩浆作用外,还有变质核杂岩、成矿作用及断陷盆地的产生。变质核杂岩在120~130 Ma最为发育[41],且大部分分布在克拉通北缘。在华北克拉通发育了两条近南北向的岩浆−矿床带,岩浆−成矿作用年龄分别集中在140~102 Ma和135~100 Ma。在中国东部的大型金矿成矿作用出现在125~120 Ma[48,49],其与吴福元等[41]研究认为金属金矿床形成在125 Ma左右的一个狭窄的时间范围内,以及翟明国[50]研究认为

表3 苏红图火山岩同位素

Table 3 Isotopes of Suhongtu volcanic rocks

样品号	$^{206}Pb/^{204}Pb$	2SE(M)%	$^{207}Pb/^{204}Pb$	2SE(M)%	$^{207}Pb/^{204}Pb$	2SE(M)%	$^{87}Sr/^{86}Sr$	(2σ)	$^{143}Nd/^{144}Nd$	(2σ)
sht-06	17.9368	0.015	15.4832	0.016	38.1678	0.018	0.706611	0.000012	0.512457	0.000015
sht-08	17.8987	0.009	15.4818	0.010	38.1503	0.010	0.706782	0.000008	0.512475	0.000015
sht-11	17.9089	0.011	15.4831	0.012	38.1483	0.013	0.705867	0.000012	0.512480	0.000015
sht-18	17.8307	0.011	15.4916	0.012	37.4447	0.013	0.707098	0.000014	0.512318	0.000014
sht-23	17.8386	0.011	15.4689	0.012	37.9882	0.011	0.705498	0.000010	0.512471	0.000015
sht-28	17.8309	0.020	15.4745	0.023	38.0358	0.030	0.705477	0.000012	0.512445	0.000016

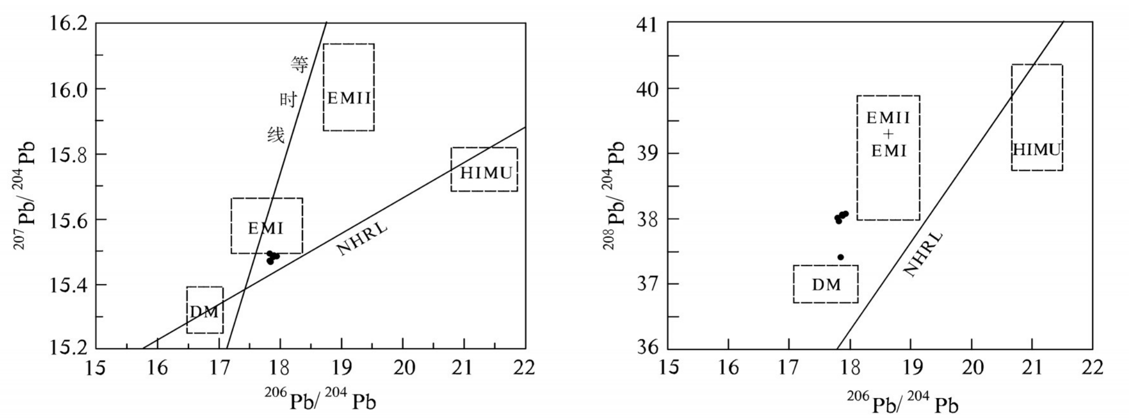

图9 火山岩$^{206}Pb/^{204}Pb-^{207}Pb/^{204}Pb$与$^{206}Pb/^{204}Pb-^{208}Pb/^{204}Pb$关系图解[26]

EMI、EMII—富集地幔端元;DM—亏损地幔同位素组成范围;HIMU—高U/Pb地幔组成范围;NHRL—北半球参考线

Fig. 9 Pb isotopic compositions of Suhongtu volcanic rocks$^{206}Pb/^{204}Pb$ versus$^{207}Pb/^{204}Pb$ and $^{206}Pb/^{204}Pb$ versus $^{208}Pb/^{204}Pb$[26]

EMI−Type I enriched mantle, EMII−Type II enriched mantle; DM−Range of depleted mantle isotopic composition; HIMU−Range of high U/Pb ratio mantle; NHHRL−Northern hemisphere reference line

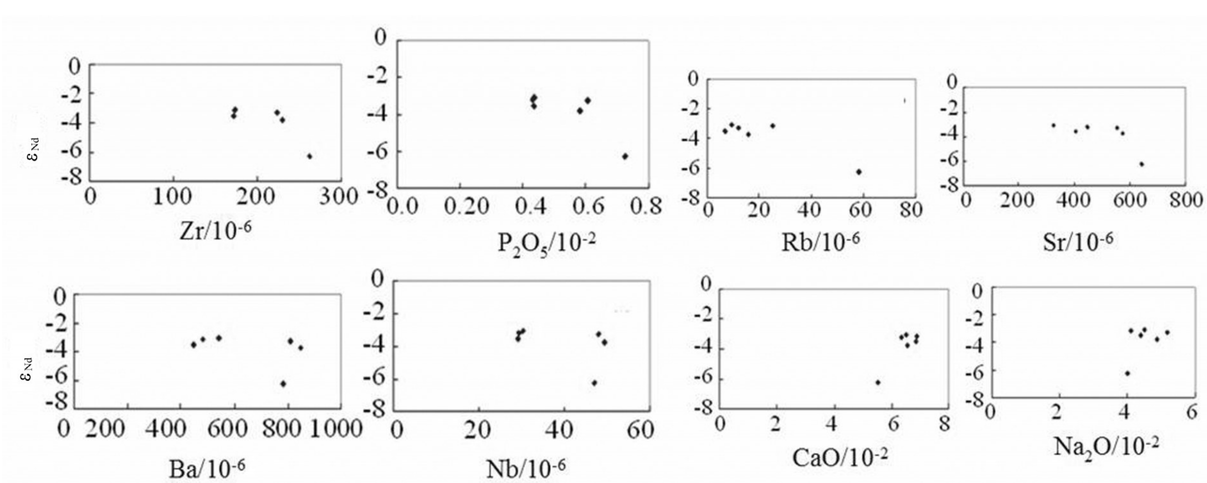

图10 苏红图火山岩$\varepsilon_{Nd}(t)$与Zr、P_2O_5、Rb、Sr、Ba、Nb、CaO、Na_2O关系图

Fig.10 Diagram showing relationships between $\varepsilon_{Nd}(t)$ and Zr, P_2O_5, Rb, Sr, Ba and Nb for volcanic rocks of Suhongtu depression

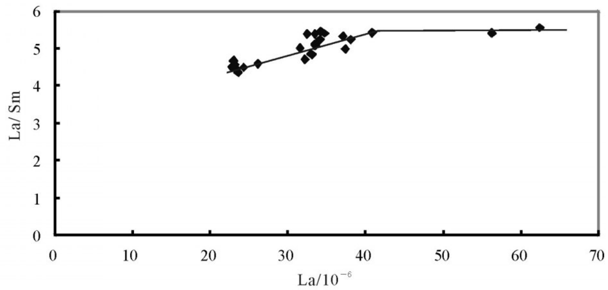

图11 La−La/Sm关系图
Fig.11 Diagram showing relationship between w(La)/w(Sm) and La

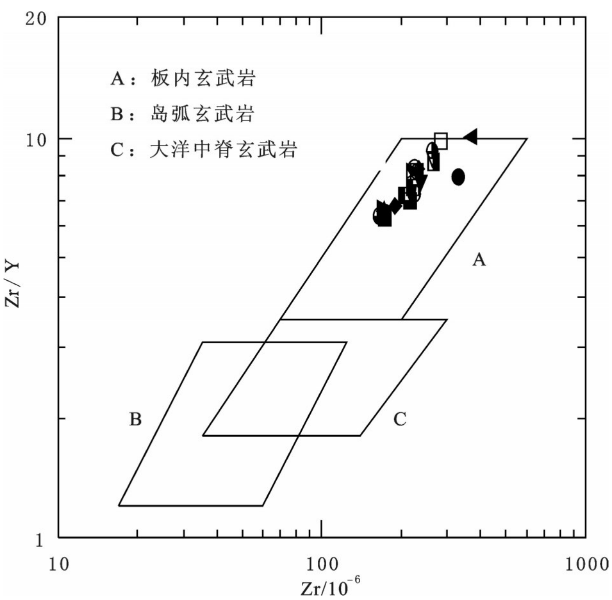

图12 Zr/Y与Zr关系图
Fig. 12 Diagram showing relationship between Zr/Y and Zr

遍布在华北东部的克拉通边缘及克拉通内部的爆发式大规模金成矿作用主期在(120±10) Ma的结论相一致。120~140 Ma是中国东部及邻区裂陷盆地主要形成和发育时期[51]，盆地形成时代和强烈的岩浆活动、大范围的变质核杂岩和大规模成矿作用时间都相一致[52]。所以，在晚侏罗世—早白垩世时期克拉通破坏产生的浅部响应在范围上和强度上达到高峰，说明了岩石圈在此时期内遭受强烈破坏，甚至破坏达到最高峰[22]。

晚中生代—新生代，火山作用仍有分布[53−56]，但强度相对减弱(图14−e)，玄武岩以碱性和强碱性为主，且主要出现在裂谷两侧[47]。如在汾渭裂谷系北

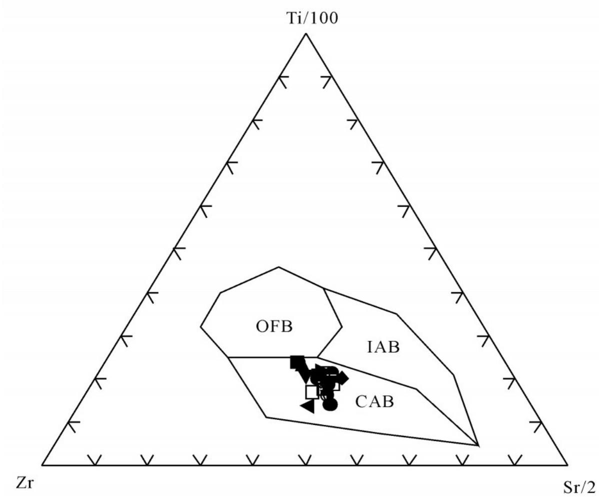

图13 Ti/100、Zr、Sr/2之间的关系图
Fig.13 Diagram showing relationships between Ti/100, Zr and Sr/2

部发现新生代玄武岩喷发，范围主要在恒山—大同及其以北地域[57]。

上述发育地壳浅部响应的区域可能也是克拉通发生破坏的区域，这些破坏区域与地震学成像结果显示的华北克拉通现今岩石圈厚度存在明显的区域差异[58−62]是相吻合的。克拉通东部广泛分布的较薄的岩石圈[58−62]以及新生代相对饱满的地幔包体地球化学特征[63−67]，反映该地区岩石圈地幔的物理和化学性质在显生宙发生了根本改变，即克拉通岩石圈已经被普遍减薄甚至发生了破坏。克拉通东部岩石圈厚度为60~100 km，向西北内部逐渐增厚至90~100 km，向克拉通内部逐渐过渡为100~150 km。同时，较薄的地壳[68−72]、较高的地表热流[73]和活跃的地震活动[74]表明，东部地壳岩石圈改造不仅横向范围广泛，而且在深度上涉及整个岩石圈。中、西部地区薄于100 km的岩石圈在河套和汾渭两个狭长的新生代局部裂陷区[24]，在银−额盆地苏红图坳陷下伏岩石圈也发生减薄，厚度仅为90 km左右[34]，其他区域岩石圈普遍厚于120 km，而在鄂尔多斯盆地之下的岩石圈厚度达200 km，且岩浆活动微弱、地热梯度低，表明了克拉通中、西部大部分地区可能保留着太古宙克拉通的核心部分。

通过克拉通破坏时在地壳浅部产生的响应对破坏时间与范围的探讨发现华北克拉通破坏的时间在空间上具有不均一性[75−77]。在石炭纪、三叠纪、

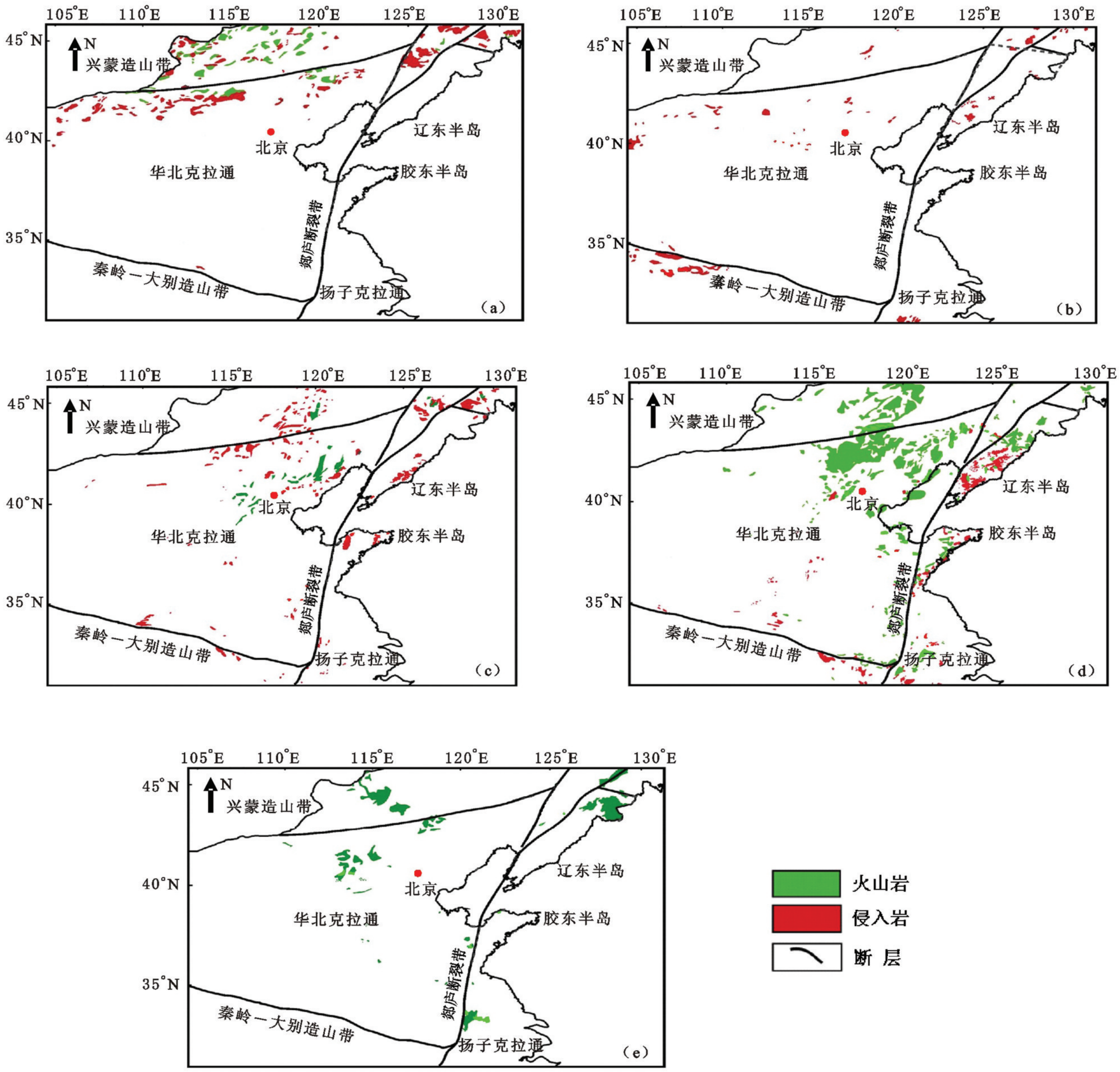

图14 晚古生代—新生代华北克拉通岩浆岩分布图[47]
a—石炭纪-二叠纪；b—三叠纪；c—侏罗纪；d—白垩纪；e—新生代
Fig.14 Distribution of NCC late Paleozoic − Cenozoic igneous rocks [47]
a−Carboniferous−Permian；b−Triassic；c−Jurassic；d−Cretaceous；e−Cenozoic

侏罗纪时发生的破坏主要集中在克拉通周缘地区，而在白垩纪则影响到了克拉通腹地，上述通过对苏红图坳陷火山岩研究得出克拉通西北缘的苏红图坳陷在早白垩世也发生了破坏。总体来说，破坏主要集中在太行山以东地区，以西的汾渭裂陷、河套裂陷与苏红图坳陷等地区发生了减薄，在地理分布上呈现出不连续的特征。

4 克拉通破坏的动力学背景与破坏机制的探讨

从华北克拉通构造纲要图中我们可以发现华北克拉通周边均为显生宙造山带所隔(图1)。克拉通北缘为古亚洲洋闭合后形成的兴—蒙造山带，南侧为著名的大别—秦岭造山带，东侧为苏鲁带和太

平洋俯冲带，克拉通中西部的河套裂陷、汾渭裂陷分别与古元古代高温变质孔兹岩带[60,61]及约18.5亿年前华北克拉通东、西部块体拼合时形成的中部造山带内[60,62]位置大致重合，而苏红图坳陷位于中亚造山带南缘，也位于两板块拼合交汇处。这些构造带在不同时期经历了重大地质事件而发生了改造。如：在晚古生代期间，克拉通北部古亚洲洋向华北克拉通俯冲，最终在二叠纪末发生了华北克拉通与蒙古地块碰撞[78]，随后，蒙古—鄂霍次克洋在晚侏罗纪中期关闭，使得华北—蒙古陆块与西伯利亚克拉通发生拼合[79,80]；晚三叠世扬子与华北板块发生了强烈碰撞[81−85]；中生代发生了太平洋板块对欧亚板块俯冲，在新生代发生了印度板块对欧亚板块[86−89]的俯冲等重大构造事件。

针对晚侏罗世—早白垩世时期，从全球来看，在早白垩世发生了大规模的海底火山活动、太平洋超级地幔柱的上升[90]与特提斯洋关闭的相关的地幔雪崩事件[91]，以及冈瓦纳大陆的裂解事件[92]。从区域来看，在中侏罗世Izanagi板块开始以4.7 cm/a的速度向东亚大陆正向俯冲，而在早白垩世初期Izanagi板块运动方向和速度突然发生改变，以30 cm/a的速度向正北方向俯冲于东亚大陆之下[93]。Kopper et al.[94,95]研究也认为自从140 Ma以来，太平洋板块向欧亚板块俯冲方向改变了多次，而最重要的一次改变是发生在120~125 Ma[94,96]，方向大致由南转变为北西方向，转幅达80°[97]。在晚侏罗世—早白垩世克拉通破坏除了可能达到峰期外，还有学者认为中国东部在该时期构造体制发生了根本的转变，侏罗纪对应于古太平洋板块相关的挤压构造环境，而白垩纪是伸展构造背景[98−101]。如：郑亚东[102]等和Davis et al.[103]对河北承德一带的构造研究表明区域内的挤压构造主要发生在127~180 Ma，而伸展作用主要发生在127 Ma以后；Tang et al.[104]通过对宁芜盆地火山岩岩浆认为，火山岩在短时间内（133~130 Ma）快速喷发而形成，暗示了中国东部早白垩世构造体制的快速转变。

研究发现克拉通破坏在石炭纪、三叠纪、侏罗纪时主要集中在克拉通周缘地区，而白垩纪则影响到了克拉通腹地。华北克拉通周缘板块碰撞拼合的时间、位置与克拉通破坏的时间、范围相吻合。那么克拉通的破坏与当时的区域构造背景甚至是全球构造背景及克拉通周缘的存在的构造带之间是否存在联系？

通过矿物物理实验和理论模拟结果显示，先前存在于岩石圈中的古老构造带在后期的热−构造事件过程中，可以引起上地幔顶部热扩散[105]和机械变形[106]的各向异性，并进一步导致岩石圈的不均匀加热和应变集中，有利于古老构造带的活化，从而使得古老岩石圈发生改造[105,107]。所以，根据克拉通破坏的时间、范围及华北地区在早白垩世发生构造体制重大转折的客观事实，结合当时全球及区域构造背景，认为二叠纪末、晚三叠世甚至新生代等时期发生在克拉通周缘的板块碰撞拼合事件使得先前存在的古老构造带的活化，造成岩石圈发生破坏。而在晚侏罗世—早白垩世初期，处于全球构造背景中的太平洋板块在对亚欧板块俯冲过程中，全球构造事件导致太平洋板块俯冲速度与方向发生重大变化，致使华北克拉通构造体制发生重大转折，从而造成了华北克拉通东部在早白垩世发生了强烈破坏，甚至达到了破坏峰期。

所以，克拉通周缘的构造薄弱带的俯冲、碰撞与华北克拉通破坏关系极为密切，它们可能对华北克拉通破坏产生了重要影响[108−110]，构造薄弱带的位置可能就是岩石圈减薄的起始位置，并且它们的俯冲与碰撞的时间是华北克拉通破坏的起始时间，从而最终导致了克拉通的破坏在时空上存在不一致性[75−77]。

5 结 论

西伯利亚板块、内蒙古褶皱带和华北地块在晚侏罗世碰撞拼合，导致华北克拉通西北部苏红图坳陷下伏岩石圈减薄，随着岩石圈地幔的减薄，在早白垩世（105~113 Ma）该区下伏软流圈地幔岩浆上涌，在上涌的过程中没有经历地壳物质的明显混染，经平衡部分熔融及随后的分离结晶共同作用形成了陆内苏红图高钾火山岩。

华北克拉通破坏在石炭纪、三叠纪、侏罗纪时主要集中在克拉通周缘地区，而白垩纪则影响到了克拉通腹地。克拉通破坏范围主要发生在太行山东部地区，太行山以西的河套裂陷、汾渭裂陷发生了减薄，而苏红图坳陷在早白垩世也发生减薄，破坏范围分布在地理上呈不连续分布特征，造成这种分布特征的主要原因是由于在克拉通周缘先前存

在的构造薄弱带受到了后期构造活动的改造,改造导致了岩石圈的破坏,从而导致了克拉通的破坏在时空上存在不一致性。

致谢: 在野外工作的还有浙江油田的张磊、胜利油田的禚元杰、中国石油大学(华东)研究生王安东、大庆油田王金华、孟玮等,在成文过程中得到了中科院广州地化所郭锋研究员的无私帮助,广西地质调查局的覃晓峰博士在火山岩分析方面给予了无私帮助,中国科学院地质与地球物理研究所的老师对火山岩进行了精心的分析测试,在此一并表示感谢!

参考文献(References):

[1] 刘春燕, 林畅松, 吴茂炳, 等. 银根—额济纳旗中生代盆地构造演化及油气勘探前景[J]. 中国地质, 2006, 33(6): 1328−1335.

Liu Chunyan, Lin Changsong, Wu Maobing, et al. Tectonic evolution and petroleum prospects of the Mesozoic Inggen−Ejin Qi basin, Inner Mongolia[J]. Geology in China, 2006, 33(6): 1328−1335(in Chinese with English abstract).

[2] 周波, 金之钧, 王毅, 等. 塔里木盆地台盆区火山作用对有机质演化的影响[J]. 石油学报, 2007, 28(6): 17−20.

Zhou Bo, Jin Zhijun, Wang Yi, et al. Effect of igneous intrusion on evolution of organic matters in Tarim Basin[J]. Acta Petrolei Sinica, 2007, 28(6): 17−20(in Chinese with English abstract).

[3] 孙永革, 傅加谟, 刘德汉, 等. 火山活动对沉积有机质演化的影响及油气地质意义——以辽河盆地东部凹陷为例[J]. 科学通报, 1995, 40(11): 1019−1022.

Sun Yongge, Fu Jiamo, Liu Dehan, et al. Effects of volcanic activity on organic evolution and its petroleum geological significance: Taking eastern Liaohe basin as an example[J]. Chinese Science Bulletin, 1995, 40(11): 1019−1022(in Chinese).

[4] 任收麦, 朱日祥, 黄宝春, 等. 造山带内古地磁研究——以苏宏图早白垩世火山岩为例[J]. 中国科学(D)辑, 2002, 10: 799−804.

Ren Shoumai, Zhu Rixiang, Huang Baochun, et al. The Paleomagnetism study of orogenic belt——Take early Cretaceous volcanic rocks in Suhongtu as an example[J].Science in China (Series D), 2002, 10: 799−804 (in Chinese)

[5] 钟福平, 钟建华, 王毅, 等. 银−额盆地苏红图坳陷早白垩世火山岩对阿尔金断裂研究的科学意义[J]. 地学前缘, 2011, 18(3): 233−240.

Zhong Fuping, Zhong Jianhua, Wang Yi, et al. The Early Cretaceous volcanic rocks of Suhongtu Depression in Inggen−Ejin Qi Basin: Its scientific significance to the research of Altun fault[J]. Earth Science Frontiers, 2011, 18(3): 233− 240 (in Chinese with English abstract)

[6] 钟福平, 钟建华, 王毅, 等. 银根—额济纳旗盆地苏红图坳陷早白垩世火山岩地球化学特征与成因[J]. 矿物学报, 2014, 34(1): 107−116.

Zhong Fuping, Zhong Jianhua, Wang Yi, et al. Geochemistry characteristics and origin of early Cretaceous volcanic rocks in Suhongtu depression, Inner Mongolia, China[J]. Acta Mieralogica Sinica, 2014, 34(1): 107−116(in Chinese with English abstract)..

[7] 钟福平, 钟建华, 由伟丰. 银根—额济纳旗盆地苏红图坳陷早白垩世火山岩幔源特征[J]. 地质学报, 2011, 85(11): 2003−2013.

Zhong Fuping, Zhong Jianhua, You Weifeng. Characteristics of the Early Cretaceous mantle− derived volcanic rocks in the Suhongtu Depression of Inggen− Ejin Qi Basin[J]. Acta Geologica Sinica, 2011, 85(11): 2003−2013(in Chinese with English abstract).

[8] 翁文灏. 中国东部中生代以来之地壳运动及火山活动[J]. 中国地质学会志, 1927, 6: 9−37

Wong Wenhao. Crustal movements and igneous activities in eastern China since Mesozoic time[J]. Geological Society of China, 1927, 6, 9−37(in Chinese with English abstract).

[9] 陈国达. 中国地台"活化区"的实例并着重讨论华夏古陆问题[J]. 地质学报, 1956, 36: 239−272.

Chen Guoda. Examples of "activizing region" in the Chinese platform with special reference to the "cathaysia" problem[J]. Acta Geologica Sinica, 1956, 36, 239− 272(in Chinese with English abstract).

[10] 邓晋福, 肖庆辉, 邱瑞照, 等. 华北地区新生代岩石圈伸展减薄的机制与过程[J]. 中国地质, 2006, 33(4): 751−761.

Deng Jinfu, Xiao Qinghui, Qiu Ruizhao, et al. Cenozoic lithospheric extension and thinning of North China: Mechanism and process[J]. Geology in China, 2006, 33(4): 751− 761(in Chinese with English abstract).

[11] Menzies M A, Fan W M, Zhang M. Palaeozoic and Cenozoic lithoprobes and the loss of >120 km of Archaean lithosphere, Sino− Korean Craton, China[C]//Prichard H M, Alabaster T, Harris N B W, et al, (eds.). Magmatic Processes and Plate Tectonics. Geol Soc Special Publ., 1993, 76: 71−78.

[12] 邓晋福, 莫宣学, 赵海玲, 等. 中国东部岩石圈根/去根作用与大陆"活化"[J]. 现代地质, 1994, 8(3): 349−356.

Deng Jinfu, Mo Xuanxue, Zhao Hailing, et al. Lithosphere root/ de− rooting and activation of the east China continent[J]. Geoscience, 1994, 8(3): 349− 356(in Chinese with English abstract).

[13] Xu Y G. Thermo−tectonic destruction of the Archean lithospheric

keel beneath eastern China: Evidengc, timing and mechanism[J]. Phys. Chem. Earth, 2001, 26: 747−757.

[14] 朱日祥, 郑天瑜. 华北克拉通破坏机制和古元古代板块构造体系[J]. 科学通报, 2009, 54: 1950−1961.
Zhu Rixiang, Zheng Tianyu. Destruction geodynamics of the North China Craton and its Paleoproterozoic plate tectonics[J]. Chinese Sceinec Bulletin, 2009, 54(5): 1950−1961(in Chinese with English abstract).

[15] 李洪颜, 徐义刚, 黄小龙, 等. 华北克拉通北缘晚古生代活化: 山西宁武—静乐盆地上石炭统太原组碎屑锆石U−Pb测年及Hf同位素证据[J]. 科学通报, 2009, 54: 632−640.
Li Hongyan, Xu Yigang, Huang Xiaolong, et al. Activation of northern margin of the North China Craton in late Palaozoic: evidence from U−Pb dating and Hf isotopes of detrital zircons from the Upper Carboniferous Taiyuan formation in the Ningwu−jingle basin[J]. Chinese Sceinec Bulletin, 2009, 54(5), 632−640 (in Chinese).

[16] Zhang S H, Zhao Y, Song B, et al. Carboniferous granitic plutons from the northern margin of the North China block: Implications for a late Palaeozoic active continental margin[J]. J. Geol. Soc. London, 2007, 164: 451−463.

[17] Yang J H, Sun J F, Chen F K, et al. Sources and petrogenesis of late Triassic dolerite dikes in the Liaodong Peninsula: Implications for post−collisional lithosphere thinning of eastern North China Craton[J]. J. Petrol., 2007, 48: 1973−1997.

[18] 韩宝福, 加加美宽雄, 李惠民. 河北光头山碱性花岗岩的时代、Nd−Sr同位素特征及其对华北早中生代壳幔相互作用的意义[J]. 岩石学报, 2004, 20: 1375−1388.
Han Baofu, Kagami Hiroo, Li Huimin. Age and Nd−Sr isotopic geochemistry of the Guangtoushan alkaline granite, Hebei Province, China: implications for early Mesozoic crust−mantle interaction in North China Block[J]. Acta Petrologica Sinica, 2004, 20, 1375−1388(in Chinese with English abstract).

[19] Gao S, Rudnick R L, Carlson R W. Re−Os evidence for replacement of ancient mantle lithosphere beneath the North China Craton[J]. Earth Planet Sci. Lett., 2002, 198: 307−322.

[20] Gao S, Rudnick R L, Yuan H L, et al. Recycling lower continental crust in the North China craton[J]. Nature, 2004, 432: 892−897.

[21] Griffin W L, Zhang A D, O'Reilly S Y. Phanerozoic evolution of the lithosphere beneath the Sino−Korean Craton[J]. Am. Geophys. Union Geodyn. Ser., 1998, 100: 107−126.

[22] Wu F, Lin J, Wilde S, et al. Nature and significance of the Early Cretaceous giant igneous event in eastern China[J]. Earth Planet. Sci. Lett., 2005, 233: 103−119.

[23] 路凤香, 郑建平, 邵济安, 等. 华北东部中生代晚期—新生代软流圈上涌与岩石圈减薄[J]. 地学前缘, 2006, 13(2): 86−92.
Lu Fengxiang, Zheng Jianping, Shao Jian, et al. Asthenospheric upwelling and lithospheric thinning in late Cretaceous−Cenozoic in eastern North China[J]. Earth Sicence Forntiers, 2006, 13(2): 86−92(in Chinese with English abstract).

[24] 朱日祥, 徐义刚, 朱光, 等. 华北克拉通破坏[J]. 中国科学: (D辑), 2012, 42 (8): 1135−1159.
Zhu Rixiang, Xu Yigang, Zhu Guang, et al. Destruction of the North China Craton[J]. Science in China (Series D), 2012, 42 (8): 1135−1159(in Chinese).

[25] Zindler A, Hart S R. Chemical Geodynamics[J]. Ann. Rev. Earth and Planetary Science Letters, 1986, 14: 493−571.

[26] 章邦桐, 吴俊奇, 凌洪飞, 等. 会昌早白垩世橄榄粗玄岩(shoshonite)成因的元素及Sr−O−Nd−Pb同位素地球化学证据[J]. 地质学报, 2008, 82(7): 986−997.
Zhang Bangtong, Wu Junqi, Ling Hongfei. Geochemical evidence of element and Sr−O−Nd−Pb isotopes for petrogenesis of the Huichang Early Cretaceous shoshonite, southern Jiangxi province [J]. Acta Geologica Sinica, 2008, 82(7): 986−997(in Chinese with English abstract).

[27] Zhao X X, Che R S, Zhou Y X, et al. New paleomagnetic results from North China: Collision and suturing with Siberia and Kazakastan [J]. Tectonophysics, 1990, 181: 43−81.

[28] 方大钧, 王朋岩, 沈忠悦, 等. 塔里木地块新生代古地磁结果及显生宙视极移曲线[J]. 中国科学(D辑), 1998, 28(增刊): 90−96.
Fang Dajun, Wang Pengyan, Shen Zhongyue, et al. The result of paleomagnetism of Cenozoic era and the apparent polarwander path of phanerozoic eons in Tarim block[J]. Science in China (Series D), 1998, 28(Supp.): 90−96(in Chinese).

[29] 朱日祥, 杨振宇, 吴汉宁, 等. 中国主要地块显生宙古地磁视极移曲线与地块运动[J]. 中国科学(D辑), 1998, 28(增刊): 1−16.
Zhu Rixiang, Yang Zhenyu, Wu Hanning, et al. The Apparent Polarwander Path of Paleomagnetism of Phanerozoic Eons and Block Movement of Major Blocks of China[J].Science in China (Series D), 1998, 28(Supp.): 1−16(in Chinese).

[30] Huang B C, Otofuji Y, Yang Z, et al. New Silurian and Devonian palaeomagnetic results from the Hexi Corridor terrane, Northwest China and their tectonic implication [J]. Geophys. J. Int., 2000, 140(1): 132−146.

[31] Zhao X, Coe R, Gilder S A, et al. Palaeomagnetism constrains on the palaeography of China: implications for Gondwanaland [J]. Aust. J. Earth Sci., 1996, 3: 643−672.

[32] 万渝生, 伍家善, 耿元生. 碱性玄武岩形成的时限及其地质意

义[J]. 地球学报, 1995, 16(4): 365−372.

Wan Yushneg, Wu Jiashan, Geng Yuansheng. The time limit of formation of alkaline basalts and its geological signifance[J]. Acta Geoscientia Sinica, 1995, 16(4): 365− 372(in Chinese with English abstract).

[33] 靳久强, 孟庆任, 张研. 额济纳旗地区侏罗—白垩纪盆地演化与油气特征[J]. 石油学报, 2000, 21(4): 13−21.

Jin Jiuqiang, Meng Qingren, Zhang Yan. Evolution and Hydrocarbon features of the Jurassic and Cretaceous basins, Ejinaqi[J]. Acta Petrolei Sinica, 2000, 21(4): 13− 19(in Chinese with English abstract).

[34] 邱瑞照, 李廷栋, 周肃, 等. 中国大陆岩石圈物质组成及演化[M]. 北京: 地质出版社, 2006.

Qiu Ruizhao, Li Tingdong, Zhou Su, et al. Material Composition and Evolution of the Chinese Continental Lithosphere[M]. Beijing: Geological Publishing House, 2006(in Chinese with English abstract).

[35] Zhang S H, Zhao Y, Song B, et al. Carboniferous granitic plutons from the northern margin of the North China block: Implications for a late Palaeozoic active continental margin[J]. J. Geol. Soc. London, 2007, 164: 451−463.

[36] Chen J F, Xie Z, Li H M, et al. U−Pb zircon ages for a collision−related K−rich complex at Shidao in the Sulu ultrahigh pressure terrane[J]. China Geochem. J., 2003, 37: 35−46.

[37] Xie Z, Li Q Z, Gao T S. Comment on "Petrogenesis of post−orogenic syenites in the Sulu orogenic belt, east China: Geochronological, geochemical and Nd−Sr isotopic evidence" by Yang et al[J]. Chem. Geol., 2006, 235: 191−194.

[38] Xu W L, Wang D Y, Liu X C, et al. Discovery of eclogite inclusion and its geological significance in early Jurassic intrusive in Xuzhou, northern Anhui, eastern China[J]. Chinese Science Bulletin, 2002, 47: 1212−1217.

[39] Xu W L, Gao S, Wang Q H, et al. Mesozoic crustal thickening of the eastern North China Craton: Evidence from eclogite xenoliths and petrologic implications[J]. Geology, 2006, 34(9): 721−724.

[40] 许文良, 杨承海, 杨德彬, 等. 华北克拉通东部中生代高Mg闪长岩——对岩石圈减薄机制的制约[J]. 地学前缘, 2006, 13(2): 120−129.

Xu Wenliang, Yang Chenghai, Yang Debin, et al. Mesozoic high−Mg diorites in eastern North China craton: constraints on the mechanism of lithospheric thinning[J]. Earth Sicence Forntiers, 2006, 13(2): 120−129(in Chinese with English abstract).

[41] 吴福元, 徐义刚, 高山, 等. 华北岩石圈减薄与克拉通破坏研究的主要学术争论[J]. 岩石学报, 2008, 24(6): 1145−1174.

Wu Fuyuan, Xu Yigang, Gao Shan, et al. Lithospheric thinning and destruction of the North China Craton[J]. Acta Petrologica Sinica, 2008, 24(6): 1145− 1174 (in Chinese with English abstract).

[42] Wu F Y, Yang J H, Wilde S A, et al. Geochronology, petrogenesis and tectonic implications of Jurassic granites in the Liaodong Peninsula, NE China[J]. Chem. Geol., 2005, 221: 127−156.

[43] Charles N, Gumiaux C, Augier R, et al. Metamorphic Core Complexes vs. synkinematic plutons in continental extension setting: Insights from key structures (Shandong Province, eastern China) [J]. J. Asian Earth Sci., 2011, 40: 261−278.

[44] Zhang X H, Mao Q, Zhang H F, et al. A Jurassic peraluminous leucogranite from Yiwulüshan, western Liaoning, North China Craton: Age, origin and tectonic significance[J]. Geol. Mag., 2008, 145: 305−320.

[45] Yang D B, Xu W L, Wang Q H, et al. Chronology and geochemistry of Mesozoic granitoids in the Bengbu area, central China: Constraints on the tectonic evolution of the eastern North China Craton[J]. Lithos, 2010, 114: 200−216.

[46] Jiang Y H, Jiang S Y, Ling H F, et al. Petrogenesis and tectonic implications of Late Jurassic shoshonitic lamprophyre dikes from the Liaodong Peninsula, NE China[J]. Miner Petrol, 2010, 100: 127−151.

[47] 徐义刚, 李洪颜, 庞崇进, 等. 论华北克拉通破坏的时限[J]. 科学通报, 2009, 54: 1974−1989.

Xu Yigang, Li Hongyan, Pang Chongjin, et al. On the timing and duration of destruction of the North China Craton[J]. Chinese Sci. Bull., 2009, 54: 1974−1989(in Chinese with English abstract).

[48] Li, Q L, Chen F K, Wang, X L, et al. Ultra−low procedural blank and the single−grain mien Rb−Sr isochron dating[J]. Chin. Sci. Bull., 2005, 50: 2861−2865.

[49] Yang J H, Zhou X H. Rb−Sr, Sm−Nd, and Pb isotope systematics of pyrite: Implications for the age and genesis of lode gold deposits[J]. Geology, 2011, 29: 711−714.

[50] 翟明国. 华北克拉通的形成演化与成矿作用[J]. 矿床地质, 2010, 29(1): 24−36.

Zhai Mingguo. Tectonic evolution and metallogenesis of North China Craton[J]. Mineral Deposits, 2010, 29(1): 24− 36 (in Chinese with English abstract).

[51] 张岳桥, 赵越, 董树文, 等. 中国东部及邻区早白垩世裂陷盆地构造演化阶段[J]. 地学前缘, 2004, 11(3): 123−133.

Zhang Yueqiao, Zhao Yue, Dong Shuwen, et al. Tectonic evolution stages of the Early Cretaceous rift basin in Eastern

China and adjacent areas and their geodynamic background[J]. Earth Sicence Forntiers, 2004, 11(3): 123−133(in Chinese with English abstract).

[52] Ren J Y, Tamaki K, Li S T, et al. Late Mesozoic and Cenozoic rifting and its dynamic setting in Eastern China and adjacent areas[J]. Tectonophysics, 2002, 344: 175−205.

[53] Guo F, Fan W M. & Li C W. Geochemistry of late Mesozoic adakites from the Sulu belt, eastern China: magma genesis and implications for crustal recycling beneath continental collisional orogens[J]. Geological Magazine, 2006, 143, 1−13.

[54] Fan W M, Guo F, Wang Y J, et al. Geochemistry of late Mesozoic volcanism in the northern Huaiyang belt, central China: partial melts from a lithospheric mantle with subducted continental crust relicts beneath the Dabie orogen[J]. Chemical Geology, 2004, 209, 27−48.

[55] Guo F, Fan W M, Wang Y J, et al. Geochemistry of late Mesozoic mafic rocks in west Shandong Province: characterizing the lost lithospheric mantle beneath North China Block[J]. Geochemical Journal, 2003, 37, 67−73.

[56] Guo F, Fan W M, Wang Y J, et al. Late Mesozoic mafic intrusive complexes in North China Block: Constraints on the nature of subcontinental lithospheric mantle[J]. Physics and Chemistry of the Earth (A), 2001, 26, 759 −771.

[57] 邢作云, 赵斌, 涂美义, 等. 汾渭裂谷系与造山带耦合关系及其形成机制研究[J]. 地学前缘, 2005, 12(2): 247−262.

Xing Zuoyun, Zhao Bin, Tu Meiyi, et al. The formation of the Fenwei rift valley[J]. Earth Science Frontiers, 2005, 12(2): 247−262(in Chinese with English abstract).

[58] Chen L, Zheng T Y, Xu W W. A thinned lithospheric image of the Tanlu Fault Zone, eastern China: Constructed from wave equation based receiver function migration[J]. J. Geophys Res, 2006, 111: B09312, doi: 10.1029/2005JB003974.

[59] Chen L, Wang T, Zhao L, et al. Distinct lateral variation of lithospheric thickness in the Northeastern North China Craton[J]. Earth Planet. Sci. Lett., 2008, 267: 56−68.

[60] Chen L. Lithospheric structure variations between the eastern and central North China Craton from S− and P− receiver function migration[J]. Phys. Earth Planet. Inter, 2009, 173: 216−227.

[61] Chen L, Cheng C, Wei Z G. Seismic evidence for significant lateral variations in lithospheric thickness beneath the central and western North China Craton[J]. Earth Planet Sci Lett, 2009, 286: 171−183.

[62] Chen L. Concordant structural variations from the surface to the base of the upper mantle in the North China Craton and its tectonic implication[J]. Lithos, 2010, 120: 96−115.

[63] 刘翠, 邓晋福, 张贵宾, 等. 华北地区新生代岩石圈伸展减薄机制的数值模拟[J]. 中国地质, 2006, 33(4): 885−895.

Liu Cui, Deng Jinfu, Zhang Guibin, et al. Numerical simlation of the mechanism of Cenozoic lithospheric extension− thinning in North China[J]. Geology in China, 2006, 33(4): 885− 895 (in Chinese with English abstract).

[64] Fan W M, Zhang H F, Baker J, et al. On and off the North China Craton: Where is the Archaean keel?[J] J Petrol, 2000, 41: 933−950.

[65] Xu Y G. Thermotectonic destruction of the Archean lithospheric keel beneath Eastern China: Evidence, timing, and mechanism[J]. Phys Chem Earth A, 2001, 26: 747−757.

[66] Wu F Y, Lin J Q, Simon A W, et al. Nature and significance of the Early Cretaceous giant igneous event in Eastern China[J]. Earth Planet Science Letters, 2005, 233: 103−119.

[67] Menzies M A, Xu Y G, Zhang H F, et al. Integration of geology, geophysics and geochemistry: A key to understanding the North China Craton[J]. Lithos, 2007, 96: 1−21.

[68] Li S L, Mooney W D, Fan J C. Crustal structure of mainland China from deep seismic sounding data[J]. Tectonophysics, 2006, 420: 239−252.

[69] Zheng T Y, Chen L, Zhao L, et al. Crust− mantle structure difference across the gravity gradient zone in the North China Craton: Seismic image of the thinned continental crust[J]. Phys. Earth Planet. Inter., 2006, 159: 43−58.

[70] Zheng T Y, Chen L, Zhao L, et al. Crustal structure across the Yanshan Belt at the northern margin of the North China Craton[J]. Phys Earth Planet Inter, 2007, 161: 36−49.

[71] Zheng T Y, Zhao L, Xu W W, et al. Insight into modification of North China Craton from seismological study in the Shandong Province[J]. Geophys Res Lett, 2008, 35: L22305, doi: 10.1029/2008GL035661.

[72] Zheng T Y, Zhao L, Zhu R X. New evidence from seismic imaging for subduction during assembly of the North China Craton[J]. Geology, 2009, 37: 395−398.

[73] Hu S B, He L J, Wang J Y. Heat flow in the continental area of China: A new data set[J]. Earth Planet Science Letters, 2000, 179: 407−419.

[74] Kusky T M, Windley B F, Zhai M G. Tectonic evolution of the North China Block: From orogen to craton to orogen[J]. Geological Society, London, Special Publications, 2007, 280: 1−34.

[75] Zheng J P, Griffin W L, O'Reilly S Y, et al. Mineral chemistry of

peridotites from Paleozoic, Mesozoic and Cenozoic lithosphere: constraints on mantle evolution beneath Eastern China[J]. J. Petrol., 2006, 47: 2233−2256.

[76] Zheng J P, Griffin W L, O'Reilly S Y, et al. Mechanism and timing of lithospheric modification and replacement beneath the eastern North China Craton: peridotitic xenoliths from the 100Ma Fuxin basalts and a regional synthesis[J]. Geochim. Cosmochim. Acta, 2007, 71: 5203−5225.

[77] 徐义刚. 华北岩石圈减薄的时空不均一特征[J]. 高校地质学报, 2004, 10: 324−331.
Xu Yigang. Lithospheric thinning beneath North China: a temporal and spatial perspective[J]. Geological Journal of China Universities, 2004, 10: 234−331(in Chinese with English abstract).

[78] Zhao X X, Coe R, Gilder S A. Palaeomagnetism Constrains on the Palaeography of China: Implications for Gondwanaland [J]. Aust J. Earth Sci., 1996, 3: 643−672.

[79] Xiao W, Windley B F, Hao J, et al. Accretion leading to collision and the Permian Solonker suture, Inner Mongolia, China: Termination of the central Asian orogenic belt[J]. Tectonics, 2003, 22: 1069, doi: 10.1029/2002TC001484.

[80] Zorin Y A. Geodynamics of the western part of the Mongolia−Okhotsk collisional belt, Trans−Baikal region (Russia) and Mongolia[J]. Tectonophysics, 1999, 306: 33−56.

[81] 赵子福, 郑永飞. 俯冲大陆岩石圈重熔: 大别−苏鲁造山带中生代岩浆岩成因[J]. 中国科学(D)辑, 2009, 39(7): 888−909.
Zhao Zifu, Zheng Yongfei. Remelting of subducted continental lithosphere: Petrogenesis of Mesozoic magmatic rocks in the Dabie−Sulu orogenic belt[J]. Science in China (Series D), 2009, 39(7): 888−909(in Chinese with English abstract).

[82] 郑永飞. 超高压变质与大陆碰撞研究进展: 以大别—苏鲁造山带为例[J]. 科学通报, 2008, 53(18): 2129−2152.
Zheng Yongfei. Research progress of ultrahigh pressure metamorphic and continental collision: Take Dabie− Sulu orogenic belt as an example[J]. Chinese Sceinec Bulletin, 2008, 53 (18): 2129−2152(in Chinese with English abstract).

[83] Li S G, Jagoutz E, Lo c H, et al. Sm/Nd, Rb/Sr, and Ar−Ar isotopic systematics of the ultrahigh−pressure metamorphic rocks in the Dabie−Sulu belt, Central China: A retrospcetive view[J]. Int. Geol. Rev., 1999, 41: 1114−1124.

[84] Chavagnac V, Jahn B M. Coesite−bearing eclogites from the Bixiling Complex, Dabie Mountains, China: Sm−Nd ages, geo−chemical characteristics, and tectonic implications[J]. Chem. Geol., 1996, 133: 29−51.

[85] Hacker B R, Ratschbacher L, Webb L, et al. U/Pb zircon ages constrain the architecture of the ultrahigh pressure Qinling−Dabie orogen, China[J]. Earth Planet Sci Lett, 1998, 161: 215−230.

[86] Jaeger J J, Courtillot V, Tapponnier P. Paleontological view of the ages of the Deocan traps,the Cretaceous / Tertiary boundary and the India—Asia collision[J]. Geology, 1989, 17: 316−319.

[87] Klootwijk C T, Conaghan P J, Powell C McA. The Himalayan Arc; Large−scale continental subduction orolclinal bending and back−arc spreading[J]. Earth Planet. Sci. Lett., 1985, 75: 167−183.

[88] Klootwijk C T, Gee J S, Peirce J W, Smith G M, Mc Fadden P L, An early India− Asia contact: Paleomagnetic constraints from Ninetyeast ridge, ODP leg 121[J]. Geology, 1992, 20: 395−398.

[89] Beck R A, Durbank D W, Sercomho W J, et al. Stratigraphic evidence for an early collision between northwest India and Asia[J]. Nature, 1995, 373: 55−58.

[90] Larson R L. Latest pulse of Earth: Evidence for a mid−Cretaceous superplume[J]. Geology, 1991, 19: 547−550.

[91] Machetel P, Humler E. High temperature during Cretaceous avalanche[J]. Earth Planet Sci. Lett., 2003, 208: 125−133.

[92] Wilde S A, Zhou X H, Nemchin A A, et al. Mesozoic crust−mantle beneath the North China Craton: A consequence of the dispersal of Gondwanaland and accretion of Asia[J]. Geology, 2003, 31: 817−820.

[93] Maruyama S, Suzuki Y, Kimura G, et al. Paleogeographic maps of the Japanese islands: Plate tectonic synthesis from 750Ma to the present[J]. Island Arc, 1997, 6: 121−142.

[94] Koppers A A P, Morgan J P, Morgan J W, et al. Testing the fixed hotspot hypothesis using $^{40}Ar/^{39}Ar$ age progressions along seamount trails[J]. Earth Planet. Sci. Lett, 2001, 185, 237−252.

[95] Sharp W D, Clague D A, 50−Ma initiation of Hawaiianemperor bend records major change in Pacific plate motion[J]. Science, 2006, 313, 1281−1284.

[96] Wessel P, Kroenke L. A geometric technique for relocating hotspots and refining absolute plate motions[J]. Nature, 1997, 387: 365−369.

[97] Sun Weidong, Ding Xing, Hu Yanhua, et al. The golden transformation of the Cretaceous plate subduction in the west Pacific[J]. Earth Planet. Sci. Lett., 2007, 262: 533−542.

[98] 李忠, 董仁国, 郑建平. 华北克拉通东部南北缘中生代火山−沉积格局及其构造转折过程[J]. 古地理学报, 2007, 9(3): 227−247.
Li Zhong, Dong Renguo, Zheng Jianping. Mesozoic volcanic−sedimentary configurations in north and south margins of the eastern North China Craton: Implications for tectonic transition

mechanism[J]. Journal of Palaeogeography, 2007, 9(3): 227−247 (in Chinese with English abstract).

[99] 翟明国, 孟庆任, 刘建民, 等. 华北东部中生代构造体制转折峰期的主要地质效应和形成动力学探讨[J]. 地学前缘, 2004, 11: 285−298.

Zhai Mingguo, Meng Qingren, Liu Jianming, et al. Geological features of Mesozoic tectonic regime inversion in Eastern North China and implication for geodynamics[J]. Earth Science Forntiers, 2004, 11: 285−298(in Chinese with English abstract).

[100] 李三忠, 刘建忠, 赵国春, 等. 华北克拉通东部地块中生代变形的关键时限及其对构造的制约——以胶辽地区为例[J]. 岩石学报, 2004, 20: 633−646.

Li Sanzhong, Liu Jianzhong, Zhao Guochun, et al. Key geochronology of Mesozoic deformation in the eastern block of the North China Craton and its constraints on regional tectonics: A case of Jiaodong and Liaodong Peninsula[J]. Acta Petrologica Sinica, 2004, 20(3): 633−646(in Chinese with English abstract).

[101] 陈根文, 夏换, 陈绍清. 华北地区晚中生代重大构造转折的地质证据[J]. 中国地质, 2008, 35(6): 1162−1177.

Chen Genwen, Xia huan, Chen Shaoqing. The geological evidences for the tectonic transition in late Mesozoic in North China[J]. Geology in China, 2008, 35(6): 1162− 1177(in Chinese with English abstract).

[102] 郑亚东, Davis G A, 王琮, 等. 燕山带中生代主要构造事件与板块构造背景问题[J]. 地质学报, 2000, 74(4): 289−302.

Zheng Yadong, Davis G A, Wang Zong, et al. The major Mesozoic tectonic events and the plate tectonic setting of Yanshan belt[J]. Acta Geologica Sinica, 2000, 74(4): 289− 302 (in Chinese with English abstract).

[103] Davis G A, Darby B J, Zhang Y D, et al. Geometric and temporal evolution of an extensional detachment fault, Hohhot metamorphic core complex, Inner Mongolia China[J]. Geology, 2002, 30: 1003−1006.

[104] Tang Y J, Zhang H F, Ying J F, et al., Rapid eruption of the Ningwu volcanics in eastern China: Response to Cretaceous subduction of the Pacific plate[J]. Geochem. Geophys. Geosyst., 2013, 14, 1703−1721, doi: 10.1002/ggge.20121.

[105] Tommasi A, Gibert B, Seipold U, et al. Anisotropy of thermal diffusivity in the upper mantle[J]. Nature, 2001, 411: 783−786.

[106] Tommasi A, Vauchez A. Continental rifting parallel to ancient collisional belts: An effect of the mechanical anisotropy of the lithospheric mantle[J]. Earth Planet Science Letters, 2001, 185: 199−210.

[107] Vauchez A, Barruol G, Tommasi A. Why do continents break up parallel to ancient orogenic belts?[J]. Terra Nova, 1997, 9: 62−66.

[108] Zheng J P, Griffin W L, O'Reilly S Y, et al. A refractory mantle protolith in younger continental crust, east−central China: Age and composition of zircon in the Sulu ultrahigh− pressure peridotite[J]. Geology, 2006, 34: 705−708.

[109] Zheng J P, Griffin W L, O'Reilly S Y, et al. Zircons in mantle xenoliths record the Triassic Yangtze− North China continental collsion[J]. Earth Planet. Sci. Lett., 2006, 247: 130−142.

[110] Yang J H, Wu F Y, Wilde S A, et al. Mesozoic decratonization of the North China block[J]. Geology, 2008, 36: 467−470.